HiSST: 3rd International Conference on
High-Speed Vehicle Science Technology
14 -19 April 2024, Busan, Korea

Progress in Pre-Definition of the SpaceLiner 8 Advanced Hypersonic Transport

Martin Sippel, Jascha Wilken, Leonid Bussler, Steffen Callsen, Tommaso Mauriello
Space Launcher Systems Analysis (SART), DLR, 28359 Bremen, Germany

Abstract

The SpaceLiner ultra-high-speed rocket-propelled passenger transport is in Phase A conceptual design after successful completion of the MRR. The ongoing concept evolution is addressing system aspects of the next configuration release 8. The space transportation role of the SpaceLiner concept as a TSTO-launcher is further refined and suitable precursor steps are investigated.

The SpaceLiner cabin integration is an important aspect to be addressed as well as the feasibility of performing multiple missions compliant with noise and sonic-boom constraints. The passenger capsule is currently redesigned for and integrated into the fuselage of SpaceLiner 8. The passenger and orbital stage concepts are evaluated by Multi-Disciplinary Design Analyses and Optimization.

Keywords: *SpaceLiner, RLV, Multi-Disciplinary Optimization*

Nomenclature/Acronyms

CAD	computer aided design	SLB	SpaceLiner Booster stage
CFD	Computational Fluid Dynamics	SLC	SpaceLiner Cabin
CRS	Cabin Rescue System	SLME	SpaceLiner Main Engine
DOF	Degrees of Freedom	SLO	SpaceLiner Orbiter stage
GLOW	Gross Lift-Off Mass	SLP	SpaceLiner Passenger stage
LH2	Liquid Hydrogen	SSME	Space Shuttle Main Engine
LOX	Liquid Oxygen	TPS	Thermal Protection System
MRR	Mission Requirements Review	TSTO	Two-Stage-To-Orbit
RCS	Reaction Control System	TVC	Thrust Vector Control
RLV	Reusable Launch Vehicle		

1. Introduction

The key premise behind the original concept inception is that the SpaceLiner ultimately has the potential to enable sustainable low-cost space transportation to orbit while at the same time revolutionizing ultra-long-distance travel between different points on Earth. Manufacturing and operating cost of reusable launcher hardware should dramatically shrink by regular daily launches. Current routine operations of the SpaceX Falcon9 indicates the viability of this vision.

DLR's SpaceLiner concept is similar in certain aspects to the idea of multiple-mission reusable launch vehicles. These concepts are understood to serve quite diverse missions by the same or at least a similar vehicle. The most prominent example in this category is the SpaceX Starship&SuperHeavy [1, 2]. Recently, the Starship-launch vehicle [39] has achieved significant progress in its flight testing. While in its primary role conceived as an ultrafast intercontinental passenger transport, in its second role the SpaceLiner is intended as an RLV capable of delivering heavy payloads into orbit. Currently available simulations proof that the SpaceLiner orbital version stays within the load constraints of the PAX-version which confirms feasibility of the multiple mission intention.

First proposed in 2005 [3], the SpaceLiner is under constant development and descriptions of some major updates have been published since then [4, 7 - 10, 16, 17, 23 - 28]. The European Union's 7th Research Framework Programme has supported several important aspects of multidisciplinary and

multinational cooperation in the projects FAST20XX, CHATT, HIKARI, and HYPMOCES. In the EU's Horizon 2020 program the project FALCon addressed the advanced return recovery mode "in-air-capturing" to be used by the reusable booster stage [23, 24]. The way how such hypersonic point-to-point transports like SpaceLiner are to be integrated in future controlled airspace was addressed in the SESAR-project ECHO. The SpaceLiner has been one of the reference concepts and its feasible inter-continental trajectories have been refined in dedicated analyses [23].

An important milestone was reached in 2016 with the successful completion of the Mission Requirements Review (MRR) which allows the concept to mature from research to structured development [16]. The Mission Requirements Document (MRD) [6] is the baseline and starting point for all technical and programmatic follow-on activities of the SpaceLiner Program.

Beyond the visionary technical concept, the SpaceLiner serves as source of inspiration for artists and designers. A few screenshots from the animation video are shown in Figure 1.

Figure 1: SpaceLiner mission in animated video (https://www.youtube.com/watch?v=sZYE7Bo4Elc)

2. SpaceLiner 7 architecture, geometry and main components

The arrangement of the two SpaceLiner stages, the reusable booster and the orbiter or passenger stage, at lift-off in configuration 7 is presented in Figure 2. The LOX-feedlines and the LH2-crossfeed connection attached on the booster's top outer side are visible. The feedlines of the upper stage are completely internal and ducted underneath the TPS. An adapted feedline- and crossfeed-system is needed for the LOX-tank of the TSTO orbiter stage bypassing the satellite cargo-bay (Figure 2, top).

The main dimensions of the 7-3 booster configuration are listed in Table 1 while major geometry data of the SpaceLiner 7-3 passenger or orbiter stage are summarized in Table 2.

Table 1: Geometrical data of SpaceLiner 7-3 booster (SLB) stage

length [m]	span [m]	height [m]	fuselage diameter [m]	wing leading edge angles [deg]	wing pitch angle [deg]	wing dihedral angle [deg]
82.3	36.0	8.7	8.6	82/61/43	3.5	0

Table 2: Geometrical data of SpaceLiner 7-3 passenger (SLP) / orbiter (SLO) stage

length [m]	span [m]	height [m]	fuselage diameter [m]	wing leading edge angle [deg]	wing pitch angle [deg]	wing dihedral angle [deg]
65.6	33.0	12.1	6.4	70	0.4	2.65

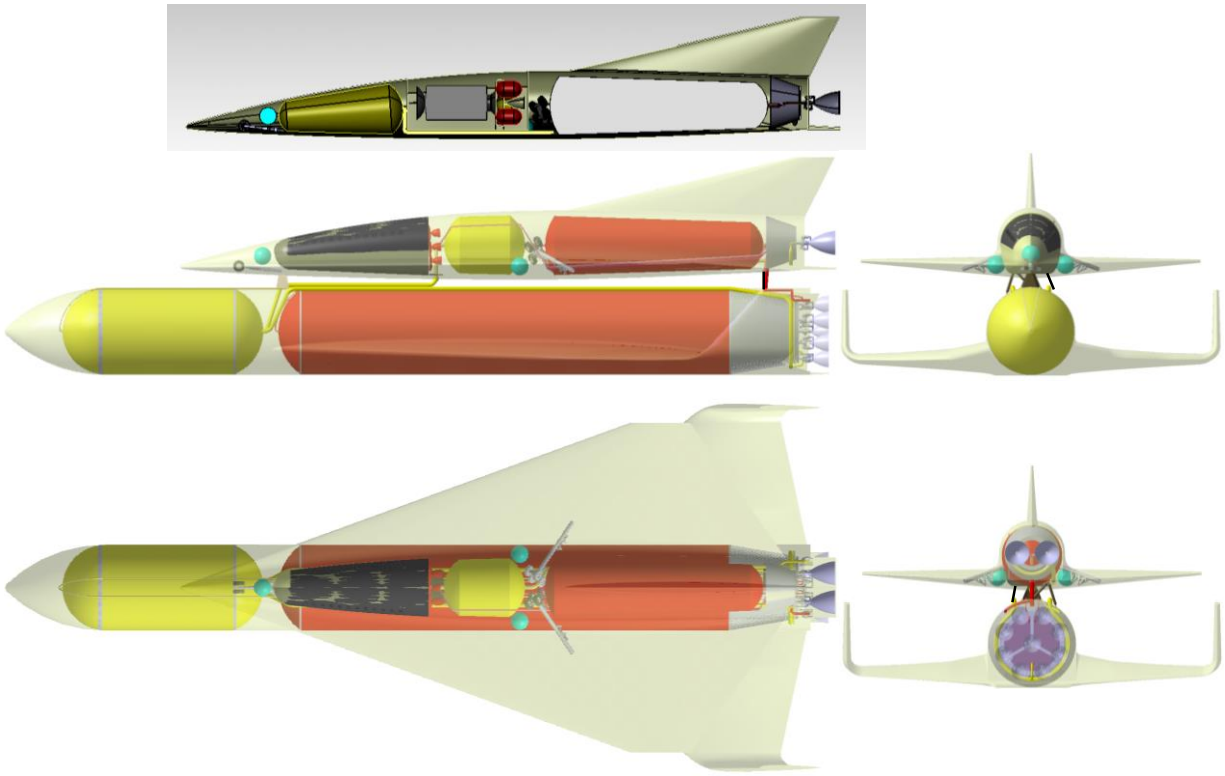

Figure 2: Sketch of SpaceLiner 7-3 launch configuration with passenger version (SLP) with its booster stage at bottom position and orbital stage of SLO in insert at top

2.1. Main propulsion system

Staged combustion cycle rocket engines with a moderate 16 MPa chamber pressure have been selected as the baseline propulsion system right at the beginning of the project [3]. A Full-Flow Staged Combustion Cycle with a fuel-rich preburner gas turbine driving the LH2-pump and an oxidizer-rich preburner gas turbine driving the LOX-pump is the preferred design solution for the SpaceLiner Main Engine (SLME). The ambitious full-flow cycle is already used by SpaceX for its Starship&SuperHeavy with the Raptor-engine [39]. This SpaceX concept is in some aspects a similar multiple mission reusable launch vehicle as SpaceLiner intends to become [9]. The Raptor engine is influenced by its interplanetary mission and hence is using a different propellant combination LOX-LCH4 which might one day be produced in-situ on Mars.

The SpaceLiner 7 has the requirement of vacuum thrust up to 2350 kN and sea-level thrust of 2100 kN for the booster engine and 2400 kN, 2000 kN respectively for the passenger stage. These values correspond to the mixture ratio of 6.5 with a nominal operational MR-range requirement from 6.5 to 5.5. The SpaceLiner 8 configuration, now under preliminary definition, keeps engine thrust at similar levels as for the SL7. These are sufficient for applications up to super heavy lift launchers and are compatible with European ground test infrastructure constraints. A partially similar staged combustion LOX/methane-engine in a range from 2000 kN up to 2500 kN is now under investigation in France under the name PROMETHEUS-X. [20]

The expansion ratios of the booster and passenger stage / orbiter SLME engines are adapted to their respective optimums; while the mass flow, turbo-machinery, and combustion chamber are assumed to remain identical in the baseline configuration [18]. Table 3 gives an overview about major SLME engine operation data for the nominal MR-range as obtained by cycle analyses [19]. Performance data are presented for the two different nozzle expansion ratios of the SpaceLiner: 33 and 59. The full pre-defined operational domain of the SLME is shown in [19] including extreme operating points.

Table 3: SpaceLiner Main Engine (SLME) technical data from numerical cycle analysis [19]

Operation point	**O1**	**O1**	**O2**	**O2**	**O3**	**O3**
Mixture ratio [-]	6		6.5		5.5	
Chamber pressure [MPa]	16		16.95		15.1	
Mass flow rate in MCC [kg/s]	513.5		555		477.65	
Expansion ratio [-]	**33**	**59**	**33**	**59**	**33**	**59**
Specific impulse in vacuum [s]	436.9	448.95	433.39	445.97	439	450.56
Specific impulse at sea level [s]	385.9	357.77	386.13	361.5	384.2	352.6
Thrust in vacuum per engine [kN]	2200	2260.68	2358.8	2427.28	2056.7	2110.49
Thrust at sea level per engine [kN]	1943	1801.55	2101.6	1967.32	1800	1651.56

Currently, the Swiss company SoftInway and DLR jointly perform a de-risk study for ESA on the SLME-rocket engine representative for the high-thrust staged-combustion type. Subcomponent sizing and definition is progressing at Phase A conceptual design level. An Integrated Power Head (Pre-burner + Turbine + Impeller pump) as it has been used on the SSME has been the preferred design solution for the SLME [18, 19]. Both preburners' external walls are actively cooled by their respective predominant fluids. The cooling fluid is heated up to subsequently used as pressurization gas for the tanks [18].

The commercial AxSTREAM® software tool for turbomachinery analyses has been implemented by SoftInway. The following turbomachinery components have been pre-designed: LPFTP pump and turbine, HPFTP pump and turbine and HPOTP pump and turbine. [19] The thermodynamic parameters of the nominal operating points are used for the turbomachines sizing and the defined pressure and MR-conditions as in Table 3 are reached.

Figure 3 shows major components of the SLME and their integration with the combustion chamber injector head and routing of the main lines. The line dimensions are adapted to massflow requirements of the cycle analyses in the full domain and stress and deformations are calculated by FEM. The preliminary sizing of the regenerative cooling of DLR [18, 19] is crosschecked with SoftInway-tools and has been locally adjusted. These ongoing activities will support the consolidation of the SLME mass balance.

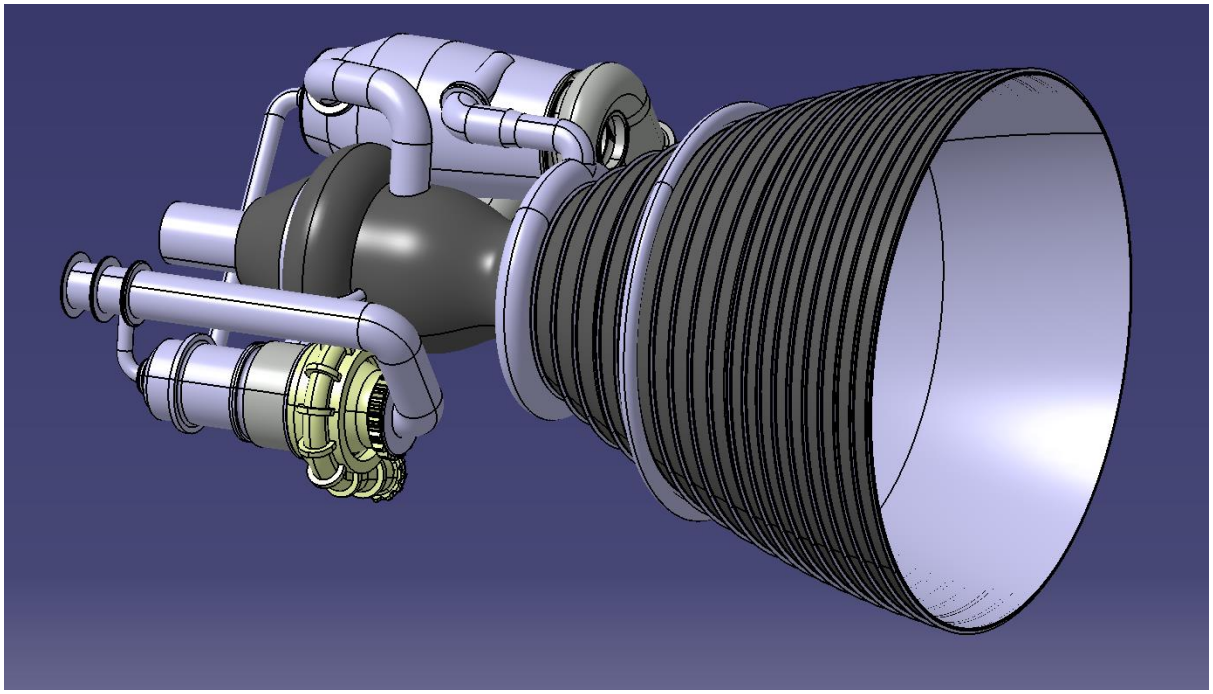

Figure 3: SLME simplified CAD geometry showing arrangement of lines and turbomachinery

An alternative architecture with oxygen-rich preburner power pack is possibly very attractive for FFSC-engines because of a compact lay-out [21] and hence significant mass savings potential. The SpaceX Raptor is using this design choice with linear arrangement of the turbopump and burner on top of the main combustion chamber. Such an architecture is under investigation for the SLME.

The principal control logic of the SLME engine is established with focus on LOX-flow and preburner mixture ratios. All controls and the actuation system are intended to be designed fully electric for maximum safety and manufacturing cost reduction. A FADEC system as in modern aircraft engines centralizes all HM-information and has a redundant data link to the vehicle's flight control and data management and data handling [18]. The HMS provides input for the engine emergency control and collection of huge operations data sets for maintenance prediction and support. Internal flow conditions, thermal and mechanical load data including vibrations can be used for automated post-flight assessment, implementing machine-learning algorithms. If such an approach is consequently followed already during development testing, a significant improvement in rocket engine reliability and robustness can be expected [19].

The size of the SLME in the smaller booster configuration is a maximum diameter of 1800 mm and overall length of 2981 mm. The larger passenger stage SLME has a maximum diameter of 2370 mm and overall length of 3893 mm. The engine masses have been previously estimated at 3375 kg with the large nozzle for the passenger stage and at 3096 kg for the booster stage [18, 19]. The ongoing engine design de-risk study will provide more refined and consistent data.

2.2. Reusable booster stage

The SpaceLiner 7 booster geometry is relatively conventional with two large integral tanks with separate bulkheads for LOX and LH2 which resembles the Space Shuttle External tank (ET) lay-out [8]. The major additions to the ET are an ogive nose for aerodynamic reasons and for housing subsystems, the propulsion system, and the wing structure with landing gear. The two tanks are part of the load carrying structure. The structure of the wing follows aircraft convention with ribs to make up the shape of the wing profile and spars to carry the main bending load [17]. Both tanks with an external structural diameter of 8.5 m carry all major loads. The interface thrust to the upper stage is going through the intertank structure right in front of the very large LH2 tank with a total internal volume of 2577 m^3. Engine thrust and the ground support loads at the launch pad are directed through the conical thrust frame which is connected to the aft-Y-ring of the hydrogen tank. The baseline structural design utilizes integrally stringer/frame stiffened aluminum lithium (Al-Li) 2195 skins for the "fuselage" (LOX & LH2 tanks, nose cone, inter-tank-structure, aft skirt), and 2195 honeycomb sandwich panels for the wings.

The booster wing (and winglet) airfoils have been selected as modified NPL-EC/ECH cut at trailing edge thickness of 75 mm [11]. The relative backward position of maximum chord thickness is beneficial for drag reduction in the supersonic and hypersonic flow (thus improved L/D) and at the same time allows for good structural efficiency where the largest aerodynamic lift forces are introduced.

Baseline recovery and return method of the reusable SpaceLiner booster stage is the patented "in-air-capturing" method which intends capturing and subsequently towing the winged vehicle using a sufficiently large subsonic aircraft. The procedure has been extensively investigated by increasingly refined simulations supported by lab-scale experiments demonstrating the high attractiveness in comparison with other recovery options (see references [22 - 25]). Despite these promising results, the dry weight of the SLB at around 200 Mg (Table 4) puts a challenge on the availability of existing airliners having adequate towing capability. This critical point is under investigation and could influence the definition of SLB8.

2.3. Reusable upper stage

The SpaceLiner7 aerodynamic shape is a result of a trade-off between the optima fulfilling the requirements of three reference trajectory points. Numerical analyses have pointed out the clear advantages of a single delta wing [11, 12]. A new, even more sophisticated optimization for the definition of the SpaceLiner 8 upper stage is ongoing and available results indicate similar tendencies (see sections 3.4 and 3.5 below!)

Major geometry data of the SpaceLiner 7-3 passenger and orbiter stage are summarized in Table 2. The SpaceLiner passenger stage's shape is shown in Figure 4.

Figure 4: SpaceLiner 7-3 passenger stage

The SpaceLiner 7 passenger stage achieves without flap deflection an excellent hypersonic L/D of 3.5 up to M=14 assuming a fully turbulent boundary layer. The laminar-turbulent transition is assumed occurring at an altitude of 58 km which is around Mach 18 [11].

In some areas of the SpaceLiner passenger stage (leading edge and nose) the heatflux and temperatures exceed those values acceptable by CMC used in the passive TPS [7, 16]. Already early in the project, transpiration cooling using liquid water has been foreseen as a potential option for solving the problem [4, 13]. In the EU-funded project FAST20XX this innovative method has been experimentally tested in DLR's arc heated facility in Cologne using subscale probes of different porous ceramic materials [14]. Test results have been scaled to full-size by heat transfer correlations and numerical assessment of the complete SpaceLiner trajectory [13]. Based on these data, a water storage tank system, a feedline manifold including control and check-valves and some bypass and redundancy lines were preliminarily sized for accommodation inside the SpaceLiner volume for which an early mass estimation was obtained [15].

Besides the overall promising results also some technical challenges of the active transpiration cooling system have been detected in the FAST20XX-investigations. Precise controllability of the water flow through the porous ceramic media has been found difficult. The experiments sometimes were running into over or under supply of water which could not be recovered within the same experimental run. A more sophisticated supply system would be needed in a flight vehicle. Another concern is the fact that the gas flow from the coolant might trigger early boundary-layer transition. As a consequence, some areas of the passive TPS might need to be reinforced. Therefore, the active transpiration cooling of leading edges and nose is still the reference design option but could once be replaced by other means of active cooling [15].

The passenger stage's internal design has been adapted for its secondary role as an unmanned satellite launcher. The passenger cabin (see separate section 2.4 below!) is not needed for this variant and is instead replaced by a large internal payload bay [16]. Key geometrical constraints and requirements are set that the SpaceLiner 7 passenger stage's outer mold line and aerodynamic configuration including all flaps should be kept unchanged. The internal arrangement of the vehicle could be adapted; however, maximum commonality of internal components (e.g. structure, tanks, gear position, propulsion and feed system) to the passenger version is preferred because of cost reflections.

Further, the payload bay should provide sufficient volume for the accommodation of a large satellite and its orbital transfer stage [8]. For this purpose, the stage's propellant loading has been reduced by 24 Mg to 190 Mg with a smaller LOX-tank to allow for a payload bay length of 12.1 m and at least 4.75 m diameter [16]. These dimensions are close to the Space Shuttle (18.3 m x 5.18 m x 3.96 m) and should accommodate even super-heavy GTO satellites of more than 8 m in length and their respective storable upper stage. Large doors open on the upper side to enable easy and fast release of the satellite payload in orbit.

The orbiter stage mass has been estimated based on the SpaceLiner 7-3 passenger stage budget (see Table 5 on p. 9). Adaptations include the complete removal of all cabin related masses. Instead a mass provision for the payload bay and its mechanisms including doors, the mounting structure, and also a radiator system for on-orbit heat-control is added. The resulting orbiter dry mass is about 102 Mg and the budget is listed in Table 6.

The aerodynamic trimming of the satellite transport stage with the existing trailing edge flaps and the bodyflap has been preliminarily checked in numerical simulation under hypersonic flow conditions of atmospheric reentry and is found feasible within the constraints of the 7-3 lay-out [16]. This promising outcome is a result of the robust SpaceLiner design philosophy which is also taking into account off-nominal abort flights. The calculated maximum L/D is reduced approximately 15% by the significant flap deflections compared to the L/D achievable for the nominal passenger mission with almost no deflection. Nevertheless, the once-around-Earth-mission of the orbiter is not compromised as demonstrated by reentry trajectory simulations [16].

2.4. SpaceLiner Cabin and Rescue System

The passenger cabin of the SpaceLiner has a double role. Providing first a comfortable pressurized travel compartment which allows for horizontal entrance of the passengers, the cabin in its second role serves as a reliable rescue system in case of catastrophic events. Thus, the primary requirements of the cabin are the possibility of being firmly attached late in the launch preparation process and fast and safely separated in case of an emergency.

The capsule should be able to fly autonomously back to Earth's surface in all separation cases. The abort trajectories are primarily influenced by the mass of the capsule and the aerodynamic performance with the most important subsystems being the separation motors, the thermal protection system (TPS), and the structure.

The SpaceLiner MRD [6, 16] defines passenger safety requirements well beyond today's reliability of launch vehicles which are nevertheless indispensable to create a viable commercial product. A safety philosophy following a multiple step approach is chosen to address the MRD-requirement:

- built-in safety and redundancy with continuous monitoring of flight critical functions and if necessary early shut-down of systems to avoid catastrophic events,
- engine-out capability during the full mission including vehicle controllability in adverse conditions [29],
- capability of the passenger stage SLP to perform abort flight maneuvers in case an early separation from the booster stage would be required during ascent,
- in case of extreme emergencies in which the previously listed safety measures are not sufficient to save life on board or can't be used anymore, the SLC will be separated and rapidly distance itself from a launch vehicle no longer controllable. Only this special case of SLC separation and its subsequent free flight conditions are relevant for the study results of this section.

Overall length of the SL7-capsule defined for 50 passengers is 15.6 m (without separation motors) and its maximum external height is 5.6 m. The estimated masses of the capsule are about 25.5 tons for the dry capsule, about 7600 kg for the passengers, crew and luggage, and 3800 kg for all propellants, separation motor, retro-rockets and RCS [17].

The capsule can be subdivided in a pressurized cabin of conical shape and an outer aerodynamic shell formed by the Thermal Protection System and which provides additional space for housing several non-pressurized subsystems [7, 16, 30]. The TPS of the SpaceLiner7 capsule is required to withstand several different heat load conditions driven by the different nominal and abort cases it might encounter. During nominal flight the capsule in its baseline design is considered to have its upper part conformal with the topside of the passenger stage (SLP). The SLC lower section is clamped within the SLP without any load carrying structural connection (see e.g. [17]) to allow rapid and safe separation in case of an emergency.

The separation motors attached to the rear end of the SpaceLiner Capsule (SLC) are of crucial importance for the capsule ejection procedure. Due to severe geometry constraints, it has been decided

early to utilize a five-motor configuration with very short cylindrical section. By the use of innovative multi-nozzle motors, expansion ratio could reach ε= 21. The maximum thrust with a chamber pressure of 15 MPa is around 856 kN at sea-level (I_{sp} = 267 s) and 908 kN (I_{sp} = 290 s) in vacuum. The total mass per motor is approximately 693 kg leading to a total mass for all motors of 3.47 tons [27, 28].

A preliminary design for the capsule's main subsystems has been elaborated [17, 31] including the body flaps, deployable rudders, the parachute system for transonic stabilization and landing, the electro-mechanical actuators and their batteries, and the reaction control system (RCS). A double bodyflap and two deployable control fins on the upper surface support flight controllability and stability. The RCS choice is characterized by 2 clusters of thrusters located in the rear part of the capsule. Each cluster provides a thrust of 3 kN along each of the double axis for a total delivered thrust of 12 kN. Parachutes are assumed to be deployed and operate in a certain altitude-Mach-box to decelerate the capsule during the final landing phase. The SpaceLiner capsule parachute system is likely a combination of supersonic stabilization chute which allows safe deceleration through the transonics and subsequent subsonic gliding by parafoil [17, 31].

Multi-body 6DOF-simulations using Simpack have been set up for the analyses of the baseline SLC integration as shown in Figure 5.

Five abort cases with SLC ejection along the nominal operational flight have been analyzed by multi-body simulations [27, 28, 33]. Initial conditions of the separation simulations have in all cases been selected from the nominal passenger flight trajectory without assuming any degradation in flight path or attitude due to anomalies.

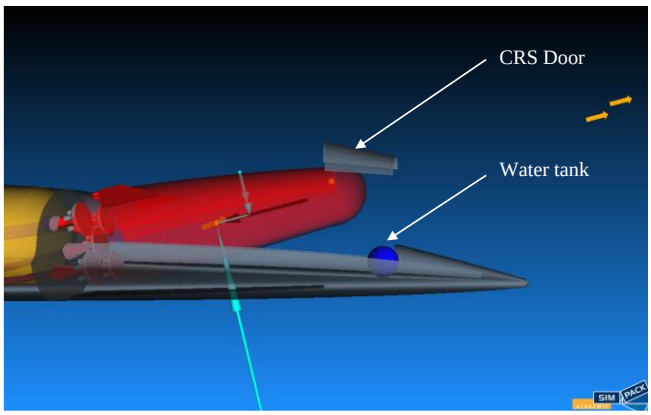

Figure 5: Simulation of SLC7 early in separation phase [33]

Obviously, this is a major simplification of potential emergency situations and is not reflecting a worst-case scenario. However, the analyses presented in [27, 28] intended to use these trade-offs to serve in the definition of system requirements in the Phase A analyses.

References 27 and 28 are presenting the axial accelerations acting on seat rows in the most forward and most aft position of the SLC depending on the separation conditions of the five cases. Around 0.4 s after initiation of the process approximately 12 g are reached in axial direction with burn duration of 2 s and in case of the aft row, very short peaks even approach up to 14 g [27, 28]. With the motors burn-out the acceleration levels are sharply reduced, nevertheless, in some cases oscillating around ±2g due to SLC rotation and the effect of aerodynamic forces. Medical investigations of NASA had demonstrated in the past that even untrained passengers will endure such elevated acceleration levels for a short time if pushed back into their seats ("eyeballs in") and somehow less in the opposite direction ("eyeballs out") corresponding here to negative n_x.

The human body is more sensitive to normal acceleration levels, pressed downward into the seats or lifted upward out of the seats, the latter corresponding to negative n_z. In case of separation at maximum dynamic pressure, the strong aerodynamic forces are influencing the acceleration profile and severe oscillations with high angular accelerations have been detected due to relatively fast rotation of the capsule [27, 28, 33]. The results clearly indicate that SLC separation at maximum dynamic pressure in transonics during ascent flight is highly critical and is not safely feasible in the current aerodynamic design of SLC7.

A preliminary assessment of the results in [27, 28] revealed that the problem is relevant for the full section of SpaceLiner flight at elevated dynamic pressure. The initial approach of actively controlling by RCS-thrusters turns out to be unfeasible at elevated dynamic pressure levels. Thrusters would have to be upscaled to an excessive size and mass. Instead the SLC needs to be redesigned for SpaceLiner 8

that its shape is aerodynamically stable or could rapidly morph into a stable configuration. Preliminary design trade-offs are discussed in section 3.6.

2.5. System masses

Based on available subsystem sizing and empirical mass estimation relationships, the stage masses have been derived as listed in Table 4 through Table 6. In case of the passenger stage (Table 5), the total fluid and propellant mass includes all ascent, residual, and RCS propellants and the water needed for the active leading edge cooling [4, 7, 15, 16]. The stages' MECO mass is approximately 151.1 Mg. The SpaceLiner 7-3's GLOW reaches about 1832 Mg (Table 7) for the reference mission Australia – Europe while the TSTO is at 1807 Mg (Table 8) still below that of the Space Shuttle STS of more than 2000 Mg.

Table 4: Mass data of SpaceLiner 7-3 booster (SLB) stage

Structure [Mg]	Propulsion [Mg]	Subsystem [Mg]	TPS [Mg]	Total dry [Mg]	Total propellant loading [Mg]	GLOW [Mg]
123.5	36.9	18.9	19.1	198.4	1272	1467

Table 5: Mass data of SpaceLiner 7-3 passenger (SLP)stage

Structure [Mg]	Propulsion [Mg]	Subsystems including cabin [Mg]	TPS [Mg]	Total dry [Mg]	Total fluid & propellant loading [Mg]	GLOW incl. passengers & payload [Mg]
55.3	9.7	43.5	22.3	129	232.1	366

Table 6: Mass data of SpaceLiner 7 Orbiter (SLO) stage (GTO mission)

Structure [Mg]	Propulsion [Mg]	Subsystems [Mg]	TPS [Mg]	Total dry [Mg]	Total fluid & propellant loading [Mg]	GLOW incl. kick-stage & payload [Mg]
60.1	9.9	9.8	22.3	102	207	309.1

Table 7: Mass data of SpaceLiner 7-3 passenger launch configuration

Total dry [Mg]	Total propellant loading [Mg]	GLOW incl. passengers & payload [Mg]
327.4	1502	1832.2

Table 8: Mass data of SpaceLiner 7-3 TSTO launch configuration

Total dry [Mg]	Total propellant loading [Mg]	GLOW incl. kick-stage & payload [Mg]
300.6	1467	1807

2.6. Reference trajectories

Possible SpaceLiner trajectories have been calculated since the early investigations started. The current configuration 7-3's flight path options are presented in references 2, 8, 9. Figure 6 shows some key-characteristics of the reference mission Australia to Europe. After its vertical take-off the 7-3-configuration is initially following a typical ascent profile of a rocket launcher. Succeeding the booster stage separation, the passenger stage is accelerated almost horizontally being the most energy-efficient way for a stage with good hypersonic L/D-ratio and intentionally long unpropelled gliding phase. Thus, second stage MECO is at slightly lower altitude than booster MECO. Axial acceleration is limited to 2.5 g which is achieved by engine throttling and subsequent engine shut-downs on the booster stage. The

short acceleration-peak at SLP MECO exceeding this limitation is an artefact of the simplified simulation and disappears when assuming a realistic engine shut-down sequence. Normal acceleration n_z is smoothly approaching 1 g during the gliding phase while axial deceleration is then around -0.1 g.

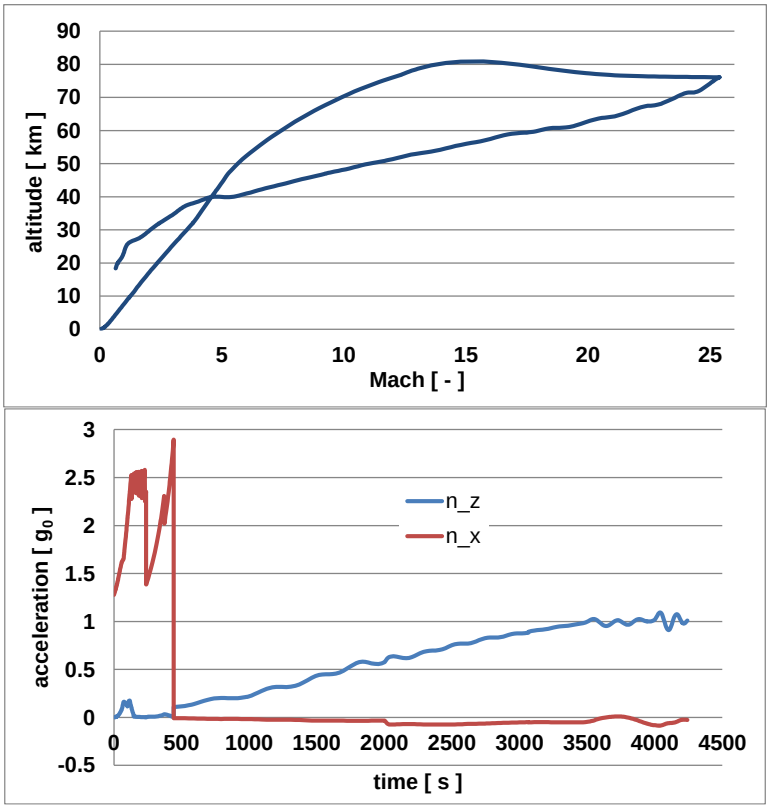

Figure 6: Calculated trajectory characteristics of SpaceLiner 7-3 reference mission Australia to Europe

Launch of the SpaceLiner 7 TSTO orbital launcher has been simulated from the Kourou space center. Reference 46 shows the Mach-altitude-profile of the reusable stages for the GTO-mission and the overall very similar behavior between passenger- and cargo reference missions in the accent segment until booster separation. The SLO is able to deliver internally more than 26150 kg of separable payload to the very low transfer orbit. Subsequently, an orbital transfer is to be used from LEO to GTO which could deliver very large communication satellites of up to 8250 kg [2, 16].

The SpaceLiner Orbiter reentry has been simulated with the result that reaching its once-around destination CSG in Kourou is without problem. The maximum heatloads remain slightly lower than for the reference passenger concept because of a different AoA-profile and lower vehicle mass. The preliminary assumption of a common TPS with the passenger stage is confirmed by the reentry simulations [2, 16, 46].

2.7. Feasible point-to-point trajectories

Beyond the reference Australia – Europe and corresponding Europe – Australia missions, other alternative intercontinental connections have been studied since the beginning of SpaceLiner investigations. Looking for suitable SpaceLiner connections between different business centers, the trajectories and related constraints were becoming more and more refined (e.g. [2, 8, 9, 16]). A systematic optimization of new point-to-point missions has been published in [22]. Numerous potential connections have been investigated for SpaceLiner 7 which are displayed on a world map in Figure 7. These all connect major economic, financial and population centers of the world. When avoiding flyover of largely populated areas as best as possible, the layout of Earth has certain limitations regarding SpaceLiner flight routes. [22]

These flight trajectories have been generated by using multi-objective optimization methods with evolutionary algorithms combining the ascent and descent phase of the flight. This methodology allows to minimize both important flight characteristics like the peak heat flux as well as the overall population

that is overflown. Consequently, the optimizer aims to move the flights towards sparsely populated areas. In general, the best areas for sparsely populated flight routes are bodies of water like the oceans. Additionally, the polar regions in the North and South are equally sparsely populated and offer the opportunity for large longitudinal crossings, for example from the Northern Atlantic to the Pacific Ocean.

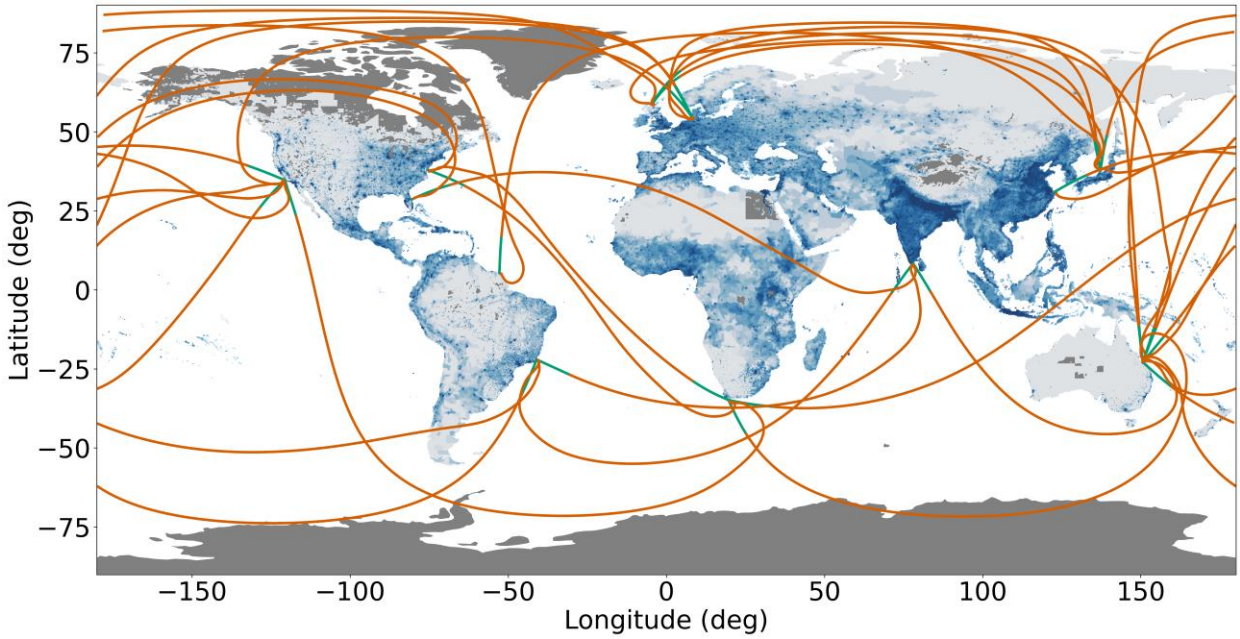

Figure 7: World map with computed potential SpaceLiner 7-3 trajectories (Green: Ascent, Orange: Descent) including population density, normalized between 1 (light-blue) and 1000 people/km^2 (dark-blue)

In contrast, when flying over land the flight routes should avoid populated areas to mitigate the effect of sonic booms on the population. This is of special concern in the northern hemisphere (Figure 8) which contains almost 90% of the population but only about two thirds of the land area.

Furthermore, the land mass and the population living there extend into higher latitudes beyond 60 degrees while in the southern hemisphere most landmasses do not extend beyond 50 degrees latitude. As a consequence, it is far easier to connect the continents in the southern hemisphere by flying over the Antarctic region and the southern Oceans. Additionally, because the Indian Ocean extends from Antarctica to India itself, even people living on landmasses in the northern hemisphere can be served with these southern-oriented flight routes [22].

Because of the launch azimuth boundaries of the chosen launch sites, it has not always been possible to have a round trip connection. A round trip connection is understood as where the flight route can be served in both directions, like the reference mission Australia – Europe.

Figure 8: Potential SpaceLiner 7-3 trajectories viewed from above the North Pole

In contrast, Australia – Florida, US is a one-way route as the flight goes around the polar region towards the East coast of the United States and Florida's launch heading range towards the east does not allow a launch back to Australia. Instead, in such a case the SpaceLiner vehicle could be imagined being part of a route system connecting multiple stops around the Earth. Here, this could for example be Australia – Florida – India – Australia as visible in Figure 7. If such multiple stops missions are attractive from the perspective of travel time saving is questionable. At least, such a connection option allows moving vehicles around the Earth and avoiding a dead end at certain commercially important locations.

Beyond the heading range boundaries, the quality of a launch site in terms of surrounding land mass as well as location on the world map is a critical factor. The chosen location in Japan is adjacent to the Sea of Japan and only allows launching towards the North to the Arctic. Thereby, it can primarily be used to connect to Europe and the northern coast of South America. However, it is not suited to launch towards other launch sites in the Pacific, which might be a disadvantage regarding the available market share. This aspect shall be further investigated in the future.

The assessments in [22] are all based on the SpaceLiner 7 and its design constraints. Range cannot be extended beyond the capabilities of the maximum propellant loading listed in Table 5 or the vehicle's geometry would need to be changed. For some missions it could be attractive "jumping over" densely populated areas by partially flying outside of the atmosphere to eliminate any sonic boom reaching ground. However, such maneuvering is hardly possible with SpaceLiner 7 because of trim constraints and changes in the aerothermal heatload environment requiring a new TPS. The redesign investigations of SpaceLiner 8 with dedicated focus on the upper or passenger stage (SLP) are trying to find a good compromise while keeping in mind feasible and attractive trajectories of a worldwide network. Results from systematic investigations are summarized in section 3.4.

3. Preliminary studies for SpaceLiner 8 and intermediate steps

3.1. SL7 improvement potential

The biplane architecture of the mated launch configuration (Figure 2) is problematic because of complex high-speed flow interactions of the two stages during ascent flight. A 6DOF-simulation based on simplified aerodynamics assuming perturbations and engine-out conditions indicates that the situation could probably be mastered by TVC [10, 17, 29]. Nevertheless, a less interacting, less complicated flow around the geometry of the ascent vehicle is desirable not least to avoid potential damage to surface insulation and coatings.

Both, the complicated flow of the launch configuration and the shock-shock interaction during booster reentry [8, 17] have motivated the investigation of potential geometry changes and improvements to the SpaceLiner booster wing geometry. A refined model of the tank, its cryogenic insulation and external TPS with an overall increased thickness has an impact on the available volume for propellants inside the SLB which is to be addressed to keep the mission margins.

Attractive methods for the return of the booster stage are to be kept in mind. The challenge of towing the large and relatively heavy SLB by existing airliners (see previous section 2.2) has an impact on the required subsonic aerodynamic performance if "in-air-capturing" is the preferred choice or, alternatively, additional propellant reserves are to be considered.

The integration of the passenger rescue system in the nose section of the upper stage and its reliable operation in all flight conditions is another critical aspect. Systematic analyses of the separation process with the SLP7 design have been performed in selected critical flight points. A summary of these results is presented in section 2.4 and reference 28 which supports a future redesign of the passenger stage.

Currently, the study for the next SpaceLiner 8 design is still ongoing and it is too early to report a consolidated configuration. However, some key results which guide future developments are presented in the following subsections.

3.2. SLB8 with small fixed wing

In order to reduce biplane flow interactions during ascent and to avoid the shock-shock-interaction on the outboard leading edge, a drastically reduced size of the SLB wing had been investigated and a sketch of the concept was presented in [8]. The relatively small wing of the so called SLB8V2 turns out to be fully sufficient for a smooth reentry avoiding extreme heatloads. However, the SLB8V2 would need to be designed for vertical downrange landing on a sea-going ship. The reentry could be somehow similar to SpaceX' Starship. After gliding deceleration to low speed and low altitude, the vehicle should rotate its attitude by 180 deg. and eventually some of the rocket engines are reignited for final slowing down to a vertical landing.

The turning maneuver of SLB8V2 before its intended vertical landing, as the procedure was assumed by DLR, has been described in [8]. The large propulsive moment required for a controlled pitch-turn maneuver was evaluated as a critical point for the feasibility of the concept [8].

Meanwhile, SpaceX has concluded several flight demonstrations with Starship prototypes at its Boca Chica site, Texas. Five subsequent test vehicles (SN8 - SN11 and SN15) were reaching at least 10000 m altitude in ascent flight before performing a controlled "sky-dive" maneuver at very low airspeed. The latter makes the major difference to the SLB8V2 assumption of aerodynamically controlled flight with dynamic pressure of at least 10 kPa. Simulations performed by DLR for the Starship returning from space [39] show that operational dynamic pressure would be rather in the range of 3 to 6 kPa, figures also supported by SpaceX' announcement. Starship is controlling its attitude by changing the dihedral deflection of both canard and main wing before rapidly performing the "belly-flop"-maneuver which rapidly brings the vehicle from almost horizontal into vertical orientation for landing. The turn is simply achieved by folding-up the aft wing and hence eliminating lift and at low dynamic pressure the TVC of three reignited SpaceX Raptor-engines controls attitude and decelerates the falling stage. Similar maneuvers were hardly achievable with the previously defined SLB8V2 as described in [8].

Although, at least the final and successful SN15 flight test of Starship can be understood as a major breakthrough, the innovative "sky-dive"- and "belly-flop"-maneuvers are highly demanding for the wing design and its control as well as the fast rocket engine reignition. Therefore, suitability of this approach also for safe and efficient operation of the SpaceLiner booster is still open for future evaluations.

3.3. SLB8 option with swept wings

As the vertical landing SLB8V2 turned out to be not fully convincing, alternative designs have been explored [8, 10]. It has been tried to maintain the promising hypersonic aerodynamic configuration with small fixed wings, however, in order to allow the stage to use "in-air-capturing" [23, 24, 25] and horizontal landing, deployable wing options have been checked on integration and mass impact [8, 10]. The challenge of this design is finding a suitable combination of different wing shapes which achieve a sufficiently high trimmed subsonic L/D of around 6, acceptable landing speed but also being fully trimable in hypersonic flight at high-angles of attack. A partially automatic variation of parameters was implemented in an MDA approach in order to systematically search for feasible and promising lay-outs shown in [10]. Instead of trailing edge flaps the inner segment had separate spoilers on its lower and upper surface.

A critical aspect for RLVs like the SpaceLiner is the selection a of reusable cryogenic tank insulation which works under multiple environmental conditions. Independent of weather conditions (e.g. temperature, humidity) effective insulation needs to be ensured and icing on the vehicle external surface is to be avoided. DLR has performed systematic research on promising combinations of insulation and reentry TPS for which the SLB7-3 serves as the reference system concept. The booster stage's reusable cryogenic tank insulation has been investigated under consideration of the external TPS by numerical simulation and experiments [36, 37, 38]. The pre-selected design option includes a so-called purge gap creating a distinct gap between the insulation of the cryogenic tank and the external thermal protection system, which has to be resistant to temperatures beyond typical limits of cryo-insulations. This relatively complex combination of external TPS and cryogenic insulation has been selected in order to avoid icing even in humid and relatively cold environment [36]. In the gap a forced flow of pre-heated dry gas is providing a controlled boundary condition at the outer interface of the cryogenic insulation. Results from the DLR projects AKIRA and TRANSIENT demonstrate the reusable

insulation concept is functioning, however, a mass impact on the SLB stage is expected [37, 38]. This effect is due to the increased weight per surface area but also by the reduced available volume for propellants inside the SLB because of the enlarged thermal protection thickness compared to the previous assumptions.

At the end of the AKIRA-project such an influence on the reference system has been investigated using the SLB8V3-variant presented in [10]. Three iteration steps were performed (see short summary in [27]) considering the definition of the thermal protection system as well as cryogenic insulation based upon AKIRA-investigations. A TPS with external metallic surface (either Inconel or Titanium or Aluminum depending on the expected maximum temperatures) has been assumed.

In the final Iteration 3 of the SLB8 design it has been decided to add an additional, 10^{th} rocket engine to improve thrust-to-weight ratio at lift-off, thus, reducing gravity losses with almost similar ascent propellant mass compared to SLB7-3. The outer dimensions of the SLB8V3 configuration in Iteration 3 are shown in [27, 46]. The fuselage diameter is increased to 8.8 m. As a consequence, the stage length reduces to 79.1 m. Aerodynamic performance requirements of the In-Air-Capturing method lead to an increased wing size. Estimated dry mass of the SLB8V3 Iteration 3 reaches 220 Mg, roughly 10% more than SLB7-3.

A systematic numerical assessment on the heatflux peaks originating from the shock-shock interaction show that these are probably less critical for the design of the outer wing leading edge than previously assumed [35] because the estimated nominal peak temperatures are excessively pessimistic. Further, trim capabilities of the large spoilers in hypersonic flow at high angles of attack are compromised by separated flowfields.

A multi-engine configuration like SLB8 with probably 10 SLME might be attractive for implementing a modular propulsion architecture in which turbomachinery power-packs are clustered separately from the thrustchambers [21]. This philosophy might improve system redundancy because in case a turbopump has to be shut-down during operations this can be compensated by the remining units. Definitely, more analyses are needed to define the SpaceLiner 8 booster stage.

3.4. Multi-disciplinary design variations in preparation of SLP8

The challenge of the passenger stage SLP8 design is to find an aerodynamic shape that allows both long-range glide missions with good hypersonic L/D, as in the case of SL7, and ballistic jumps outside the atmosphere over populated landmasses. For the latter, it is possible to eliminate all noise on the ground, but then the configuration's design needs to generate increased lift at increased AoA during re-entry to remain within acceptable heat loads.

To address these somehow contradictory requirements, a systematic variation and assessment of potential design options for the SLP8 configuration was carried-out in a multi-disciplinary approach [47]. Based on fast estimation methods the geometry of the wings has been systematically varied with regard to maximum SLP hypersonic lift-to-drag ratio, maximum trimable hypersonic lift generation as well as the resulting dry mass of the vehicle. In these analyses, other properties of the fuselage, such as the outer shape, the internal arrangement of tanks and engines and the large vertical stabilizer are still kept similar to the SLP7. Future evolutions towards a consolidated SpaceLiner 8 configuration might be extended to modifications on these items as well. Focus of the current variation is thus on the wing shape and planform while considering an improved capsule integration.

In order to identify an aerodynamic shape capable of fulfilling both the long-range missions in quasi-stationary flight as well as ballistic hops over populated landmasses a multidisciplinary design optimization methodology was established. Based on fast estimation methods (surface-inclination methods for hypersonic and handbook methods for trans- and subsonic velocities) the geometry of the orbiter wings was optimized with regard to its hypersonic lift-to-drag ratio, hypersonic lift generation as well as the resulting dry mass of the vehicle.

The shift of the CoG induced by the geometry variation was also assessed and included in generation of the pitch-trimmed aerodynamic datasets. In addition to pitch-trim other constraints such as a

maximal permissible landing speed of 100 m/s and a feasible flight path through the entire velocity regime were considered. Finally, trajectory optimizations as described in the previous section 2.7 were used to evaluate the performance of the configurations on the pareto front of the aerodynamic shape optimization.

As the assessment of the point-to-point (P2P) performance is computationally expensive, the analysis was done in two steps: First aerodynamic shapes with promising aerodynamic performances were identified through parametric studies and dedicated optimization of the aerodynamic properties and subsequently trajectory optimizations were completed only for promising configurations in order to identify the best trade-off of the aerodynamic performance metrics.

For the optimization of both, the aerodynamic properties and the trajectories, Python wrappers were used to access the DLR legacy tools used for trajectory simulation, mass modelling and aerodynamic performance computation. A genetic multi-objective algorithm from the *pymoo* [34] library was used for both optimizations, specifically the NSGA-III (Non-dominated Sorting Genetic Algorithm, version III) algorithm [44, 45]. This optimization framework has been used for all the optimization purposes in the context of SLP8 definition as it proved capable for both optimizations.

Parametric studies have been run by systematically varying the wing shape geometrical parameters and computing the associated vehicle performances. While parametric studies cannot be used to find the optimum vehicle shape, they can provide useful insights on the problem, and they can be exploited to quickly assess trends in terms of inputs-outputs or outputs-outputs interconnections. Moreover, they allow a visualization of the relative position of the previous SLP7 configuration in the design space and potentially demonstrate the progress achieved.

More than 20000 different SLP8 shape variants have been assessed by the automated MDA-process. A selection of the resulting aerodynamic parameters is presented in Figure 9. Note the SpaceLiner 7 SLP highlighted as red cross for comparison. While its trimmed L/D in hypersonic is very good and can be hardly improved (as was exactly intended in the past, see [11, 12]), the dry weight of the stage is close to the upper limit and its capability for generating high lift by increasing AoA is limited. The latter need is a driving factor in the definition of SLP8 while a weight approaching that of SLP7 would still be acceptable, it should not exceed it.

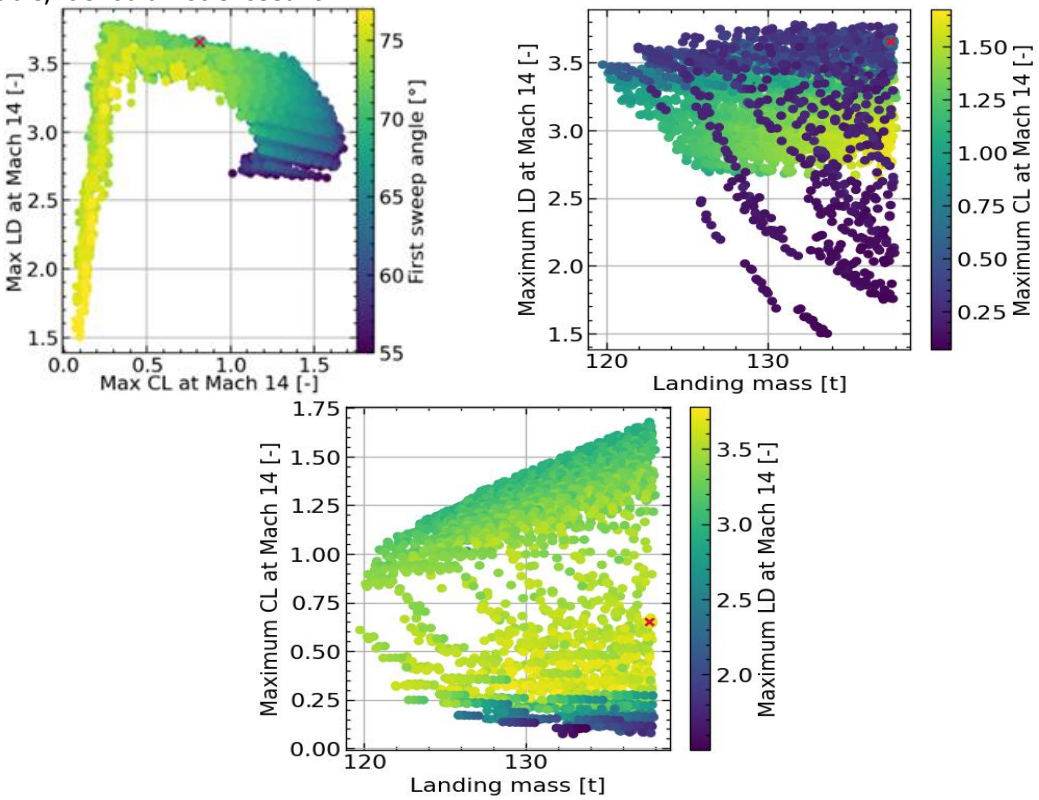

Figure 9: Results of systematic SLP8 design variations and impact on aerodynamic performance [47]

Interestingly, the SLP7 performances are located exactly in correspondence of the pareto front of max C_L – max L/D. This could be a confirmation of the SLP7 design being well performing (see section 2.3 and [12]), as well as a validation of the newly implemented optimization algorithms to accurately explore the aerodynamic shape design space.

From the results of the parametric study the following conclusions can be drawn [47]:

- The SLP7 shape is well designed as, for its value of landing mass, it is a non-dominated solution in terms of maximum C_L and maximum L/D.
- Nevertheless, considering the decremental effect that the vehicle mass has on trajectory performances, it can be expected that less massive vehicles, despite a loss in L/D or C_L, may display better trajectory performances. Moreover, less massive vehicles could still have a larger maximum C_L if the can be trimmed up to larger angles of attack.
- Parametric studies can provide useful insights, but they are not tuned to find the optimum vehicle. In fact, they explore also non-useful regions of the design space (dominated solutions), while the pareto front of the dominated solutions could be further explored with a finer resolution of the input parameters. Ultimately, these limitations are overcome by implementing a multi-objective optimization.
- When optimizing for mass, C_L and L/D, and restricting the interest to vehicles which are stable in the hypersonic regime, the additional metric of C_D, which also affects the trajectory performances, can reasonably be considered a dependent variable and it can thus be excluded from the optimization objectives.
- The hypersonic performance at Mach 14 is a good representative of the overall hypersonic performance. Allowing the subsequent vehicle optimization to focus on this case and save computational time by not simulating the entire Mach range within the optimization loop.

The process of parametric geometry variation and adaptation under several constraints (e.g. flap integration) and the generation of the related aerodynamic and performance characteristics are run fully automatic. Obtained data are post-processed and plotted similar to Figure 9. The pareto-fronts can be identified and analyzed by the stage designer to find promising design regions. These can be further checked on robustness to uncertainties, such as CoG-position, that have a significant impact on vehicle trimability and hence achievable performance. The aerothermodynamic characteristics of all promising candidates are crosschecked with OpenFoam-CFD analyses (see following section 3.5) and will be later subject to critical assessment of heatflux based on mission-optimized trajectories.

Based on the results of this initial parametric exploration, the aerodynamic shape was then optimized. The three optimization objectives were minimal dry mass, maximum L/D at Mach 14 (representative for the hypersonic reentry gliding behavior) and maximum C_L at Mach 14 (representative for elevated AoA-flight at reentry). Figure 10 shows the resulting pareto front including the maximum trimmable angle of attack. While it might appear in the three-dimensional representation that a portion of the pareto is not well explored, this is caused by a steep decrease for the objective to reach maximum C_L in that region, as the vehicles in that portion of the pareto sacrifice the ability to fly at high angles of attack for a more optimized L/D at low angles of attack.

On the right-hand side of the plot, where the pareto front is projected onto the unit simplex it can be seen that the solution space is indeed evenly explored by the NSGA-III algorithm. The right-hand side plot displays also the vehicle geometry associated to each point. It is observed that vehicles with a lower maximum trimmable angle of attack are associated to rear-shifted wings, indicating that for these types of wings the separation between CoG and CoP is larger and at angles of attack lower than 40° the maximum values of flap deflections are already reached and the vehicle cannot be trimmed at elevated AoA [47].

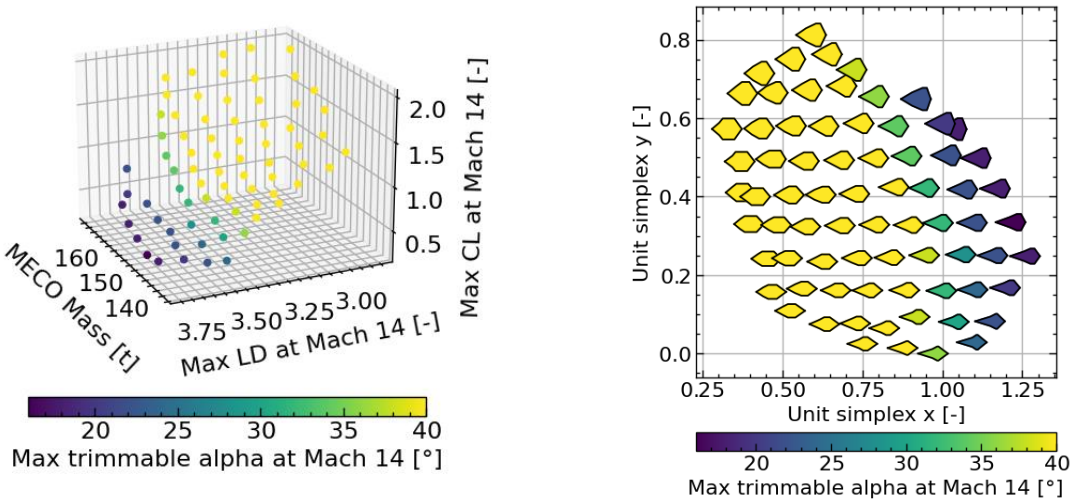

Figure 10: Variation of the maximum trimmable AoA (alpha) along the pareto surface [47]

Before the trajectory optimizations are applied to potential realistic point-to-point missions, generic trajectories launched from the equator simply in eastward, northward, and westward direction are calculated, revealing already some concepts as less attractive. For the vehicles of the pareto front of the optimized aerodynamic performance, simplified point-to-point trajectory performances were assessed for the demanding retrograde "westward launch". Therein for each case the maximum range possible at a preset maximum heat flux was optimized. Figure 11 shows exemplary results from such an optimization including five potential shapes and the resulting characteristics in 4 dimensions.

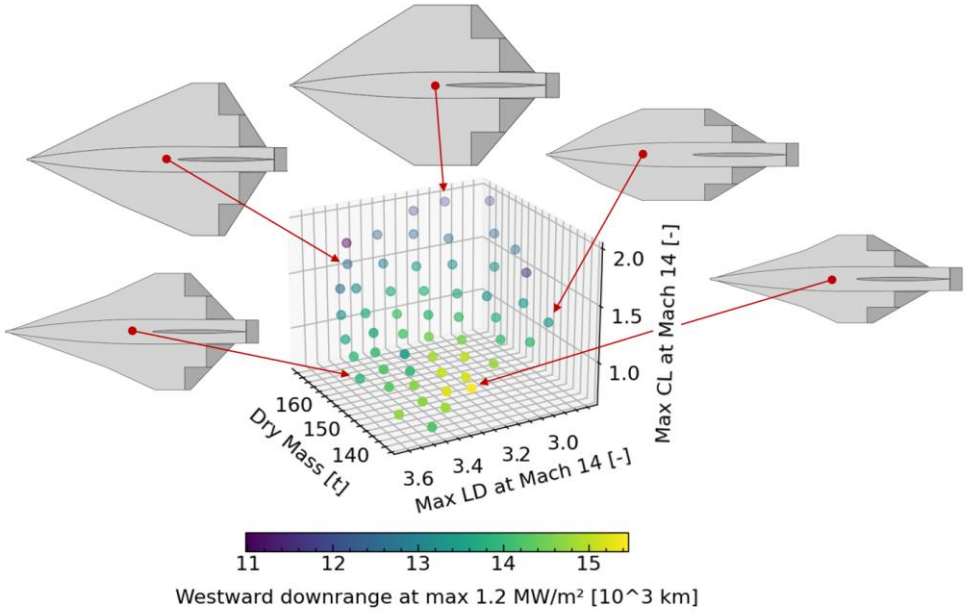

Figure 11: SLP8 design variants and resulting system characteristics

At the area of the pareto with the best P2P performance, it is limited by the landing speed constrained of 100 m/s. This indicates:

- That the maximum landing speed is the most constraining boundary, as it limits the pareto in the region where the best trajectory performances are located. It is to be expected that an increase of this constraint value could allow vehicles with even smaller wings to fly and being able to land.
- That the optimizer is working effectively, as it manages to explore the design space also in close proximity of the constrained values in order to find the most performing solutions.

As for initial parametric studies, the SLP7 configuration lies on the pareto front of the aerodynamic optimization, representing a case with a near-maximal high L/D-ratio at Mach 14. Unfortunately, its lifting capabilities are limited by the restricted trim range (the maximum trimmable angle of attack at

Mach 14 is 28°) as a consequence of the largely rear-shifted wing, while its large mass penalizes both the ascent phase and descent phase. Conversely, the best vehicles of the wing-shape optimization, even though they do not dominate the SLP7 performances, provide better tradeoffs between the three objectives (i.e. they do not sacrifice two of them to maximize a single one, which is the L/D).

The currently most promising candidate of SLP8 is designated *SLP8V-O40-0042*. Figure 12 displays the main performance metrics of this configuration. As it can be observed it is fully flyable and mostly stable in the hypersonic regime. For this reason, it can achieve good values of max C_L as a result of its large maximum angle of attack at Mach 14 (40°). This should allow new trajectories which could "jump over" populated areas to eliminate sonic boom on ground while restricting heatflux peaks due to the increased lift generation. Moreover, the required flap deflection is small at the angle of attack delivering the maximum L/D (around 8°), so that good hypersonic aerodynamic efficiency for gliding flight can be obtained as well. This combination of characteristics is exactly the kind of compromise which the systematic, multi-disciplinary investigations are aiming for SLP8.

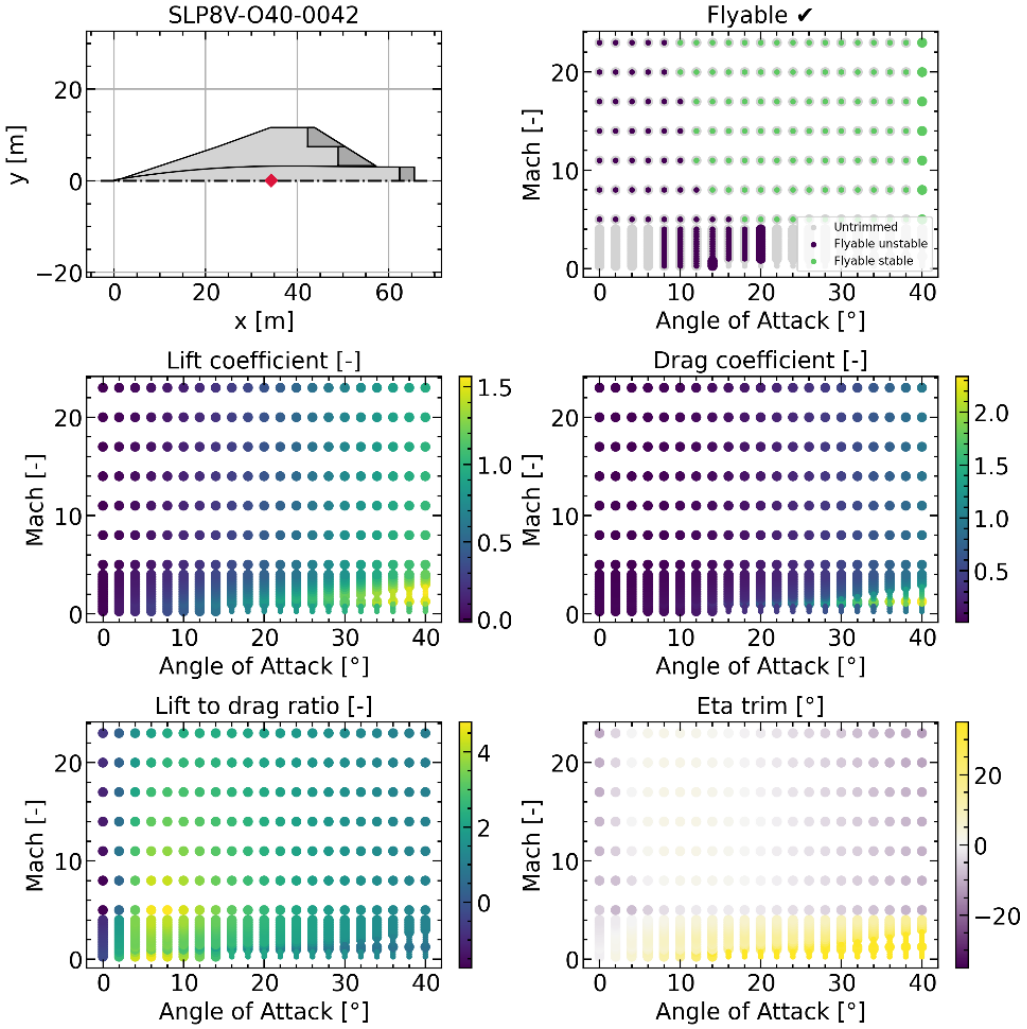

Figure 12: Preliminary aerodynamic characteristics of vehicle SLP8V-O40-0042 [47]

3.5. Summary of SLP8 variant O40-0042 status

This specific configuration evaluated in the previous section as most promising for SpaceLiner 8 shows remarkable similarities to the SLP7. However, the span is reduced and wing sweep angles are slightly adapted and as a consequence the generated lift is increased in hypersonics at elevated trimable AoA. The sensitivity of the aerodynamic characteristics to simplified modelling requires careful checks by CFD-(Euler-)methods before any configuration can be finally selected. In particular, the landing speed aerodynamics need to be considered to confirm practical feasibility of the potentially smaller size wing. Inviscid Euler calculations with the OpenFOAM environment and the steady-state, compressible

rhoSimpleFoam solver have been used. The hex-dominant meshes have been generated with the *snappyHexMesh* utility of OpenFOAM.

Some subsonic flow conditions of the SLP8 variant O40-0042 at Mach 0.5 and wing flap deflection of 10° are shown in Figure 13 and landing approach speed of Mach 0.3 in Figure 14. A leading-edge vortex on the upper surface being typical for delta wings under such conditions is clearly visible. These vortices are responsible for the additional lift at high AoA conditions and have an important effect on surface pressure distribution and hence pitch moment coefficient c_M.

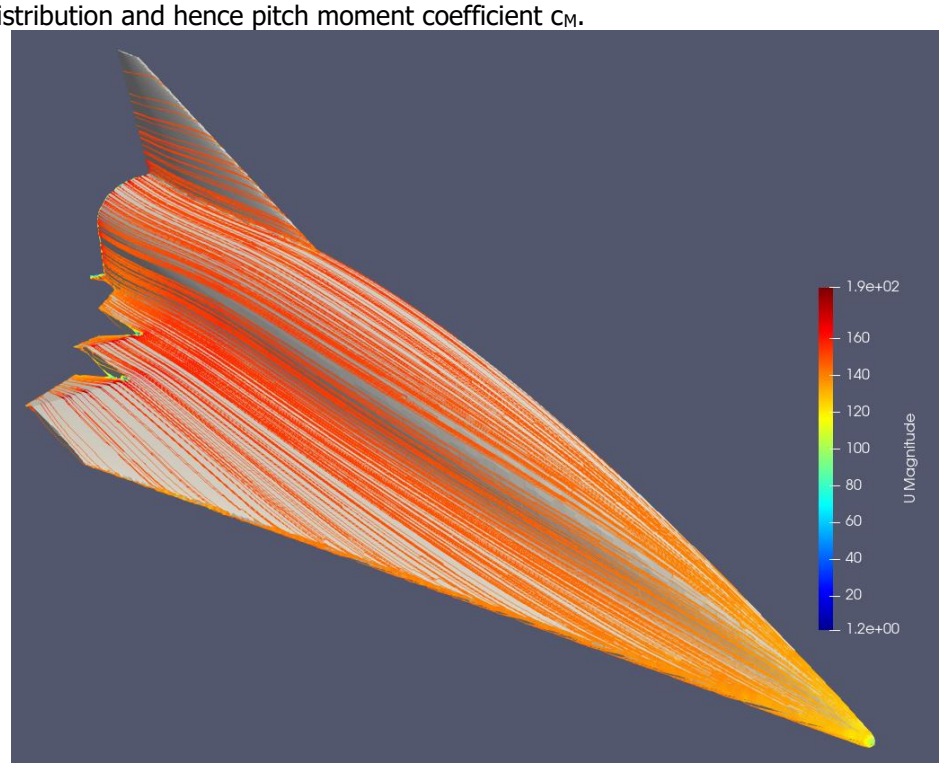

Figure 13: Velocity streamlines on SLP8 variant O40-0042 at M=0.5, AoA=0°

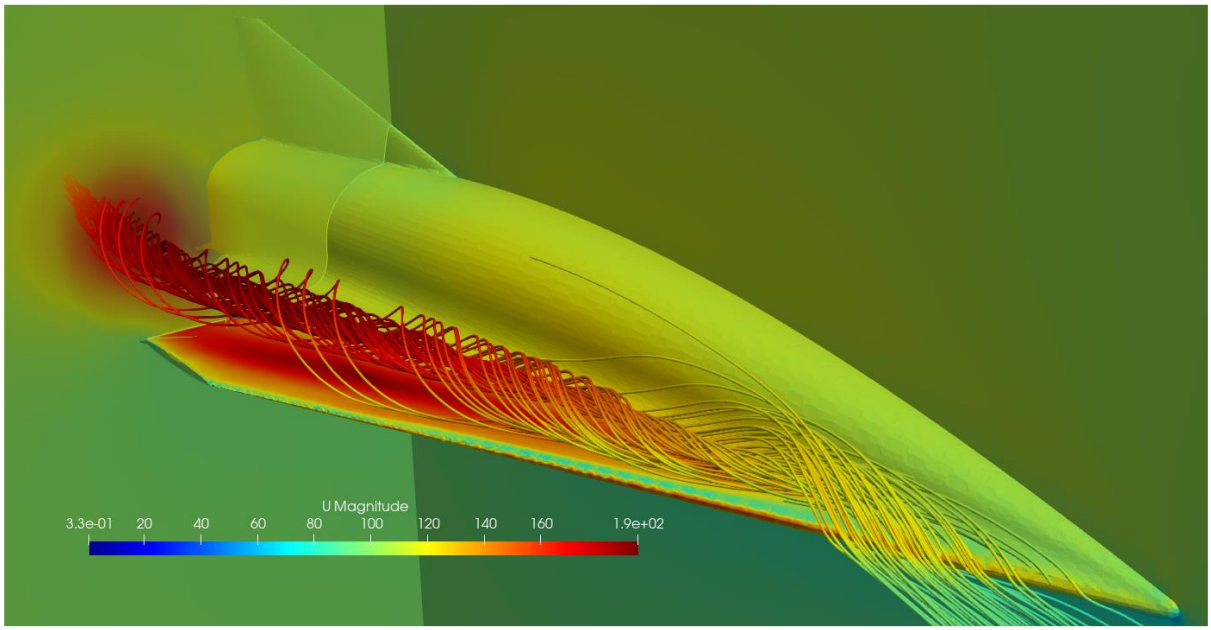

Figure 14: Computed flow field on SLP8 variant O40-0042 in subsonics close to landing conditions (M= 0.3 / AoA = 20°)

The inviscid CFD data show non-linear behavior with increasing AoA due to vortex lift and indicate significantly higher c_L coefficients at AoA beyond 10° compared with results of the fast engineering methods used in the multidisciplinary design optimization. Therefore, the feasibility of the reduced size

wing compared to SL7 is confirmed or might offer additional margins, even if viscosity effects may slightly reduce the calculated lift coefficient slope. A trimmed landing condition is reached with trailing edge flaps deflected by 10° and speed slightly below 100 m/s. The SLP8 variant O40-0042 is longitudinally unstable under current estimation of its likely CoG-position.

The external thermal protection has been preliminarily defined for the SLP8 following the SL7 pre-selection (e.g. [7, 16]). Figure 15 shows the TPS distribution on the upper and lower surface based on selected SL8 reference trajectories and subsequent iterative sizing. The windward side is protected by CMC with variable insulation thickness below while for the upper surface TABI or AFRSI has been selected similar to the Space Shuttle. A small area at the nose and leading edges including the fin needs active cooling [14, 15] and is labeled "Not defined" in Figure 15.

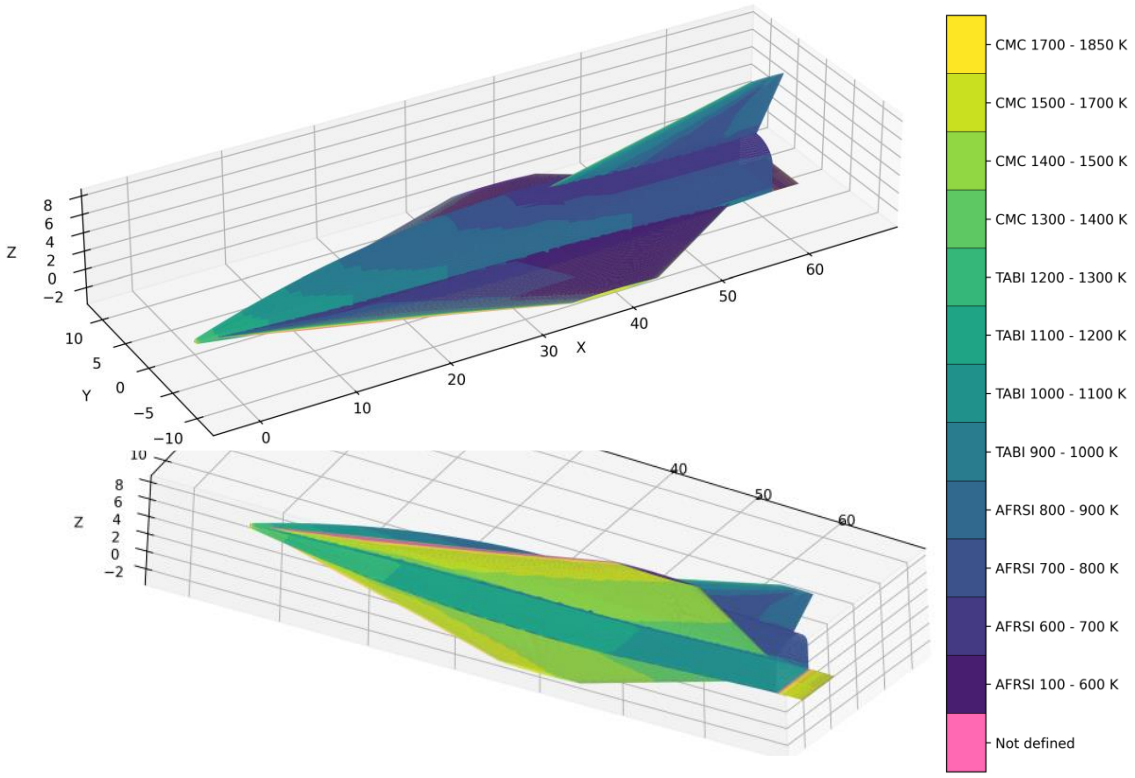

Figure 15: Preliminary distribution of TPS-types on SLP8 variant O40-0042

An essential step of the multi-disciplinary design process are trajectory optimizations similar to those described in sections 2.6 and 2.7 to evaluate the mission performance of the most promising configurations. Figure 16 presents two typical missions of SpaceLiner 8 in variant O40-0042 with different trajectory constraints. Both configurations are using the SLB8 V3 booster stage as described in section 3.3.

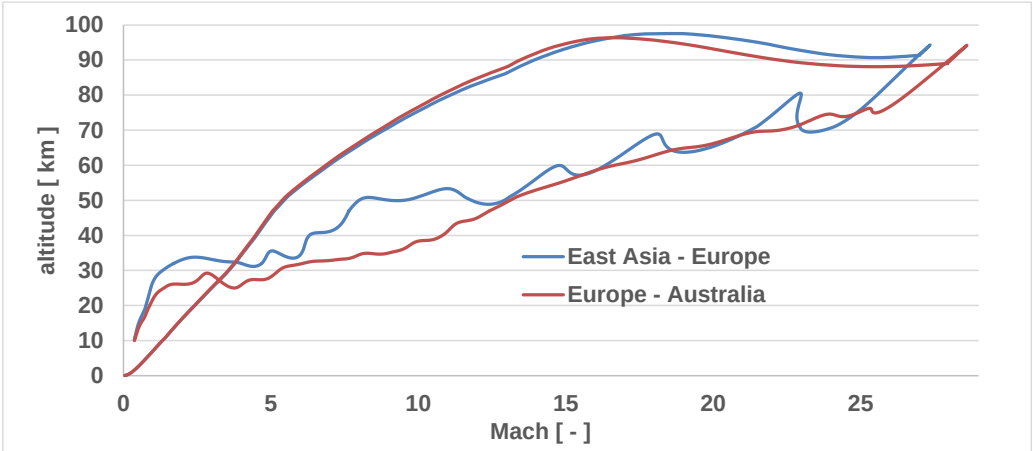

Figure 16: Calculated trajectory characteristics of SpaceLiner 8 missions East Asia to Europe and Europe to Australia

The East Asia – Europe mission is jumping over densely populated China at high altitudes to eliminate the sonic boom on ground and subsequently performs a steeper reentry. The Europe – Australia mission is following the SL7 gliding profile, although with notable differences due to the new optimization and different mass and staging characteristics of SL8. When comparing to Figure 6 it is revealed that both configurations are accelerating to slightly higher speed than SL7 (up to Mach 28.6 above 90 km) before starting the unpowered reentries. The reduced MECO mass of SLP8 O40-0042 allows for the higher velocities without violating the constraint of available propellant loading. Peak heatflux is somehow reduced compared to SL7 as the SLP8 can stay for a longer time at higher altitudes. The skips in the Asia – Europe trajectory might be eliminated in future refinements but these were not relevant in the preliminary assessment.

Although the SLP8 definition is by far not yet concluded, the current configuration SLP8 O40-0042 is a promising starting point for the next steps of investigations.

3.6. Challenges in defining SLC8 rescue capsule

The shortcomings of the SpaceLiner 7 capsule design and of its stage integration have already been discussed in the previous section 2.4. As a first measure, the "Type C" integration (schematically shown in [27, 28]) is selected as baseline which should allow a simplified and faster separation process only in the forward direction (Figure 17). Further, the architecture is now split in three sections which should be easily separable.

In a first approach, the core capsule segment is mostly similar to the previous SLC7, however, slightly shortened by about 1.5 m. The front pressure dome is the most forward point but no longer including the ablative TPS on the blunt nose. Instead a conical nose section (called LSCS) is reaching about 3.7 m to the nose and will be protected by TPS. The Liquid Separation & Control System (LSCS) comprises bi-propellant separation motors and the RCS of the stage. The new liquid separation motor is pulling the capsule in case of extreme emergencies and would reduce the number of solid separation motors at the aft end of the capsule from five to four. The LSCS tank system should feed both RCS and separation motors and as this propellant is used in the nominal mission for attitude control and liquid separation motors having a better Isp than solids, a mass saving is expected. With the RCS moved forward the aft end of the core capsule could be shortened by roughly 1 m.

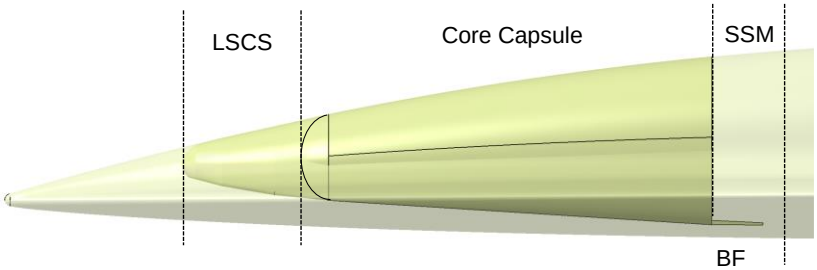

Figure 17: Potential SLP8 capsule integration concept

Behind the capsule the Solid Separation Motor (SSM) section is placed, still containing four of the solid motors as described in section 2.4 and which are shown in [27, 28]. However, the SSM is no longer directly connected with the SLC but serves structurally more the role of an interstage. This new connection should bring safety improvements as the solid motors usually remain connected with the propulsion system of SLP and only in case of extreme emergency push the SLC out of the danger zone. After a couple of seconds, the SSM should be separated and the capsule should potentially be flying in a configuration option as shown in Figure 18. After the potential reentry and most likely before parachute deployment, the LSCS will also be separated to simplify the landing of the capsule.

In Figure 18 all aerodynamic control and stability devices are presented which are currently under assessment. The deployable fins at the aft and the dual bodyflap have already been introduced with SLC7 [17]. However, this configuration could neither be stabilized nor controlled after capsule separation [27, 28]. Therefore, an aft mounted small wing had been added which, however, can't be solid structure because of integration constraints. An inflatable device is preliminarily assumed with potential synergies to studies in the Hypmoces project [17].

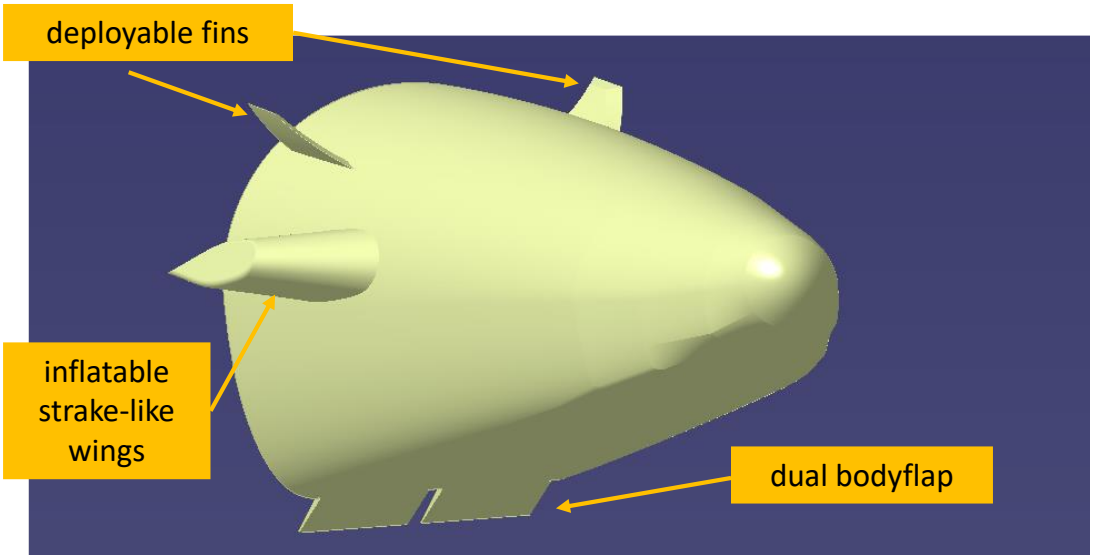

Figure 18: SLC8 external shape with LSCS attached and all potential control devices deflected

The aerodynamic concept as presented in Figure 18 or geometry variations of strake wing, bodyflap length has been subject to extensive investigations to improve the capsule's stability characteristics. Fast engineering methods in a wide range of Mach numbers and angle of attack, as well as CFD inviscid Euler calculations with the OpenFOAM environment and the compressible *rhoSimpleFoam* solver are used for selected flight points. The hex-dominant meshes are generated with the *snappyHexMesh* utility of OpenFOAM (Figure 19)

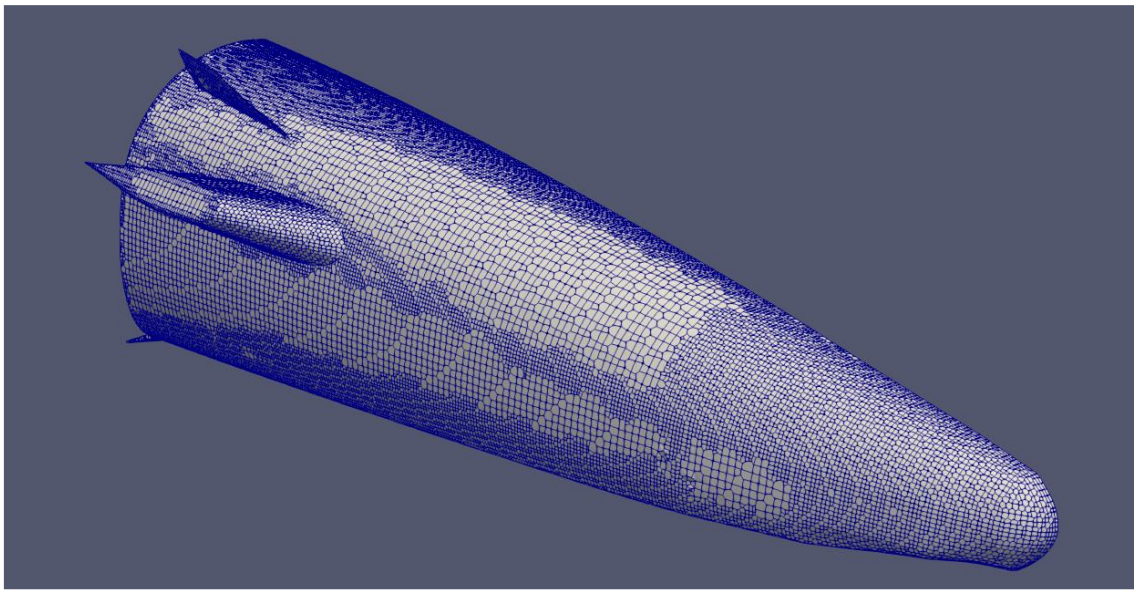

Figure 19: Surface mesh distribution on potential SLC8-geometry with deflected devices

The flow field at a flight point of M=0.5, altitude 1 km (typical for emergency separation at launch pad), AoA of 8° and body flap deflection of 20° is shown in Figure 20 with surrounding velocity streamlines.

The aerodynamic and flight dynamic assessment in the complete flight regime is not yet sufficiently fulfilling the requirement of stability and trimability. Assuming realistic CoG-positions, either the capsule is trimmed but not stable or vice versa. Up to now it has not been possible to find an aerodynamic configuration which is satisfying the requirements under the most critical elevated dynamic pressure conditions. A huge stabilizing aft cone or chute is not attractive because of the related significant drag which incapacitates the rapid distancing of the capsule in case of emergency situations. The challenge is not new for these capsule shapes and is one of the reasons why such designs have not seen practical applications to date. The shape of the SLC8 as presented in Figure 18 through Figure 20 is still preliminary and might see some, potential more radical adaptations in the future.

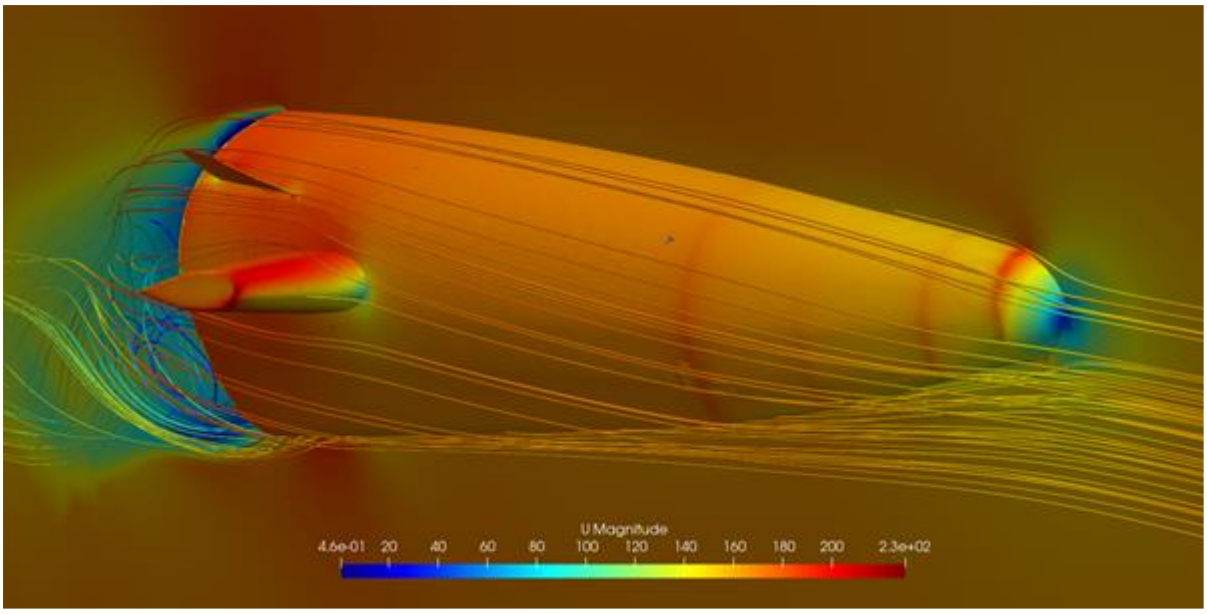

Figure 20: Velocity streamlines on potential SLC8 with control devices (M = 0.5 / AoA = 8°)

3.7. Intermediate development steps before SpaceLiner

The SpaceLiner defined as a fully-reusable, multiple-mission launch vehicle with advanced rocket engines requires mastering of ambitious technologies. The European expertise of today is limited to expendable launchers with cryogenic propulsion (Ariane 5 and 6). Directly starting the development of the SpaceLiner on such basis is risky, the more as it should also operate as a safe and commercially attractive passenger transport.

During several SpaceLiner Design Workshops potential development roadmaps have been discussed. Gaining expertise with a partially reusable space transportation system in flight operations as pure cargo carrier would be a major de-risking element before starting the commercial development of the SpaceLiner. An attractive option for such an RLV is a large reusable booster stage accelerating expendable upper stages which could be introduced as a successor to Ariane 6 after 2035.

DLR has started investigation of such launchers with the internal project name RLV-C4 [42, 46]. A systematic variation of design options on propellant choice or aerodynamic configuration has been carried-out.

4. Conclusion

The DLR proposed reusable winged rocket SpaceLiner for very high-speed intercontinental passenger transport is progressing in its conceptual design phase after having successfully completed its Mission Requirements Review (MRR). Research on the vehicle is continuously performed with support from several EC-funded projects with numerous European partners. Assuming advanced but not exotic technologies, a vertically launched rocket powered two-stage space vehicle is able to transport about 50 passengers over distances of up to 17000 km in about 1.5 hours.

Systematic optimizations of point-to-point missions connecting major economic, financial and population centers of the world have been analyzed for SpaceLiner 7 and its design constraints regarding general feasibility. Unfortunately, for the feasibility of some attractive missions, "jumping over" densely populated areas by partially flying outside of the atmosphere to eliminate any sonic boom reaching ground is hardly possible with SpaceLiner 7 because of trim constraints.

The redesign investigations of SpaceLiner 8 are trying to find a good compromise for the upper or passenger stage (SLP) while keeping in mind feasible and attractive trajectories of a worldwide network. Sophisticated, automated multi-disciplinary analyses help in finding the best compromise out of the many design choices in the definition of the upper stage. A promising configuration has been identified

with reduced size wing which still meets the landing speed constraint. Actual intercontinental point-to-point trajectories have been optimized for this variant, now representing the baseline for future design iterations.

The passenger rescue capsule, designed to be used in cases of extreme emergencies, has to be also improved which is addressed in parallel with the SpaceLiner 8 redefinition. A new, preliminary integration concept of SLC8 is presented. Various aerodynamic control and stability devices were added and varied in geometric properties. However, the aerodynamic and flight dynamic assessment in the complete flight regime is not yet sufficiently fulfilling the requirements of stability and trimability. Further modifications with potentially more radical adjustments may be required in the future.

A refined modelling of the cryo-tank's reusable insulation on the booster stage (SLB) led to an overall feasible and promising concept but also to an increase in dry weight of the stage. Adding one more SLME on the SLB is the preferred choice for version 8 which limits the overall growth of the SpaceLiner.

The SpaceLiner 8 definition is not yet completed but a technically and operationally promising approach is identified and major steps forward are evident.

Acknowledgements

The authors gratefully acknowledge the contributions of Ms. Carola Bauer, Ms. Mona Carlsen, Ms. Elena Casali, Ms. Nicole Garbers, Ms. Carina Ludwig, Ms. Sarah Lipp, Ms. Olga Trivailo, Ms. Cecilia Valluchi, Ms. Natascha Bonidis, Mr. Alexander Kopp, Mr. Arnold van Foreest, Mr. Ryoma Yamashiro, Mr. Sven Stappert, Mr. Mete Bayrak, Mr. Magni Johannsson, Mr. David Gerson, Mr. Jochen Bütünley, Mr. Sven Krummen, Mr. Tobias Schwanekamp, Mr. Sholto Forbes-Spyratos, Mr. Marco Palli, Mr. Jan-René Haferkamp, Mr. David von Rüden and Mr. Vincent Friesen to the analyses and preliminary design of the SpaceLiner.

References

1. Musk, E.: Making Life Multi-Planetary, in *NEW SPACE*, VOL. 6, NO. 1, 2018 DOI: 10.1089/space.2018.29013.emu
2. Sippel, M.; Stappert, S.; Koch, A.: Assessment of Multiple Mission Reusable Launch Vehicles, IAC-18-D2.4.04, 2018
3. Sippel, M., Klevanski, J., Steelant, J.: Comparative Study on Options for High-Speed Intercontinental Passenger Transports: Air-Breathing- vs. Rocket-Propelled, IAC-05-D2.4.09, October 2005
4. Sippel, M., Klevanski, J., van Foreest, A., Gülhan, A., Esser, B., Kuhn, M.: The SpaceLiner Concept and its Aerothermodynamic Challenges, 1st ARA-Days, Arcachon July 2006
5. Sippel, M.: Promising roadmap alternatives for the SpaceLiner, Acta Astronautica, Vol. 66, Iss. 11-12, (2010)
6. Trivailo, O. et.al.: SpaceLiner Mission Requirements Document, SL-MR-SART-00001-1/2, Issue 1, Revision 2, SART TN-005/2016, 11.07.2016
7. Sippel, M.; Schwanekamp, T; Trivailo, O; Kopp, A; Bauer, C; Garbers, N.: SpaceLiner Technical Progress and Mission Definition, AIAA 2015-3582, 20th AIAA International Space Planes and Hypersonic Systems and Technologies Conference, Glasgow, July 2015
8. Sippel, M.; Stappert, S.; Bussler, L.; Forbes-Spyratos, S.: Technical Progress of Multiple-Mission Reusable Launch Vehicle SpaceLiner, HiSST 2018-1580839, 1st HiSST: International Conference on High-Speed Vehicle Science Technology, Moscow, November 2018, Download Link
9. Sippel, M.; Stappert, S.; Koch, A.: Assessment of multiple mission reusable launch vehicles, in Journal of Space Safety Engineering 6 (2019) 165–180, https://doi.org/10.1016/j.jsse.2019.09.001
10. Sippel, M.; Stappert, S.; Bussler, L.; Singh, S.; Krummen, S.: Ultra-Fast Passenger Transport Options Enabled by Reusable Launch Vehicles, 1st FAR conference, Monopoli, September 30th – October, 3rd 2019, Download Link

11. Sippel, M.; Schwanekamp, T.: The SpaceLiner Hypersonic System – Aerothermodynamic Requirements and Design Process, 8th European Symposium on Aerothermodynamics for Space Vehicles, Lisbon, March 2015
12. Schwanekamp, T.; Bauer, C.; Kopp, A.: The Development of the SpaceLiner Concept and its Latest Progress, 4TH CSA-IAA CONFERENCE ON ADVANCED SPACE TECHNOLOGY, Shanghai, September 2011
13. Van Foreest, A.; Sippel, M.; Gülhan, A.; Esser, B.; Ambrosius, B.A.C.; Sudmeijer, K.: Transpiration Cooling Using Liquid Water, Journal of Thermophysics and Heat Transfer, Vol. 23, No. 4, October–December 2009
14. Reimer, Th.; Kuhn, M.; Gülhan, A.; Esser, B.; Sippel, M.; van Foreest, A.: Transpiration Cooling Tests of Porous CMC in Hypersonic Flow, AIAA2011-2251, 17th International Space Planes and Hypersonic Systems and Technologies Conference, 2011
15. Schwanekamp, T.; Mayer, F.; Reimer, T.; Petkov, I.; Tröltzsch, A.; Siggel, M.: System Studies on Active Thermal Protection of a Hypersonic Suborbital Passenger Transport Vehicle, AIAA Aviation Conference, AIAA 2014-2372, Atlanta, June 2014
16. Sippel, M., Trivailo, O., Bussler, L., Lipp, S., Kaltenhäuser, S.; Molina, R.: Evolution of the SpaceLiner towards a Reusable TSTO-Launcher, IAC-16-D2.4.03, September 2016, Download Link
17. Sippel, M.; Bussler, L.; Kopp, A.; Krummen, S.; Valluchi, C.; Wilken, J.; Prévereaud, Y.; Vérant, J.-L.; Laroche, E.; Sourgen, E.; Bonetti, D.: Advanced Simulations of Reusable Hypersonic Rocket-Powered Stages, AIAA 2017-2170, 21st AIAA International Space Planes and Hypersonic Systems and Technologies Conference, 6-9 March 2017, Xiamen, China, Download Link
18. Sippel, M., Wilken J.: Preliminary Component Definition of Reusable Staged-Combustion Rocket Engine, Space Propulsion 2018, Seville, May 2018, Download Link
19. Sippel, M.; Stappert, S.; Pastrikakis, V.; Barannik, V.; Maksiuta, D.; Moroz, L.: Systematic Studies on Reusable Staged-Combustion Rocket Engine SLME for European Applications, Space Propulsion 2022, Estoril, Portugal, May 2022, Download Link
20. Espinosa-Ramos, A.; Taponier, V.: Towards a new class of engine for future heavy lift launch vehicles, Aerospace Europe Conference 2023 – 10TH EUCASS – 9TH CEAS, July 2023
21. Knuth, W.; Crawford, R.; Litchford, R.: Integrated Modular Propulsion for Launch Vehicles, AlAA 93-1889, 29th Joint Propulsion Conference and Exhibit, Monterey, June 28-30, 1993
22. Sippel, M.; Bussler, L; Krause, S.; Cain, S.; Stappert, S.: Bringing Highly Efficient RLV-Return Mode "In-Air-Capturing" to Reality, HiSST 2018-1580867, 1st HiSST Conference, Moscow, November 2018
23. Sippel, M.; Singh, S.; Stappert, S.: Progress Summary of H2020-project FALCon, Aerospace Europe Conference 2023 – 10th EUCASS – 9th CEAS, Lausanne July 2023, Download Link
24. Singh, S.; Bussler, L; Bergmann, K.; Sippel, M: Mission Design and Sensitivity Analysis for In-Air Capturing of a Winged Reusable Launch Vehicle, IAC-23-D2.5.5, 74th International Astronautical Congress (IAC), Baku, Azerbaijan, 2-6 October 2023, Download Link
25. Singh, S.: Relative Navigation Implementation for the In-Air Capturing of a Winged Reusable Launch Vehicle, HiSST 2024 – 279, 3rd HiSST Conference, Busan, April 2024
26. Callsen, S.; Wilken, J.; Stappert, S.; Sippel, M: Feasible options for point-to-point passenger transport with rocket propelled reusable launch vehicles, Acta Astronautica 212 (2023) 100–110, https://doi.org/10.1016/j.actaastro.2023.07.016
27. Sippel, M., Stappert, S., Bayrak, Y.M.; Bussler, L., Callsen, S.: Systematic Assessment of SpaceLiner Passenger Cabin Emergency Separation Using Multi-Body Simulations, 2nd HiSST-conference, Bruges, September 2022
28. Sippel, M., Stappert, S., Bayrak, Y.M.; Bussler, L.: Systematic Assessment of SpaceLiner Passenger Cabin Emergency Separation Using Multi-Body Simulations, CEAS Space Journal, Vol. 15, No. 6, November 2023, published online: 02 June 2023, https://doi.org/10.1007/s12567-023-00505-z
29. Krummen, S.; Sippel, M.: EFFECTS OF THE ROTATIONAL VEHICLE DYNAMICS ON THE ASCENT FLIGHT TRAJECTORY OF THE SPACELINER CONCEPT, CEAS Space Journal, Vol. 11, Nov. 2019, pp. 161–172, https://doi.org/10.1007/s12567-018-0223-7
30. Bauer, C.; Kopp, A.; Schwanekamp, T.; Clark, V.; Garbers, N.: Passenger Capsule for the SpaceLiner, DLRK-paper, Augsburg 2014

31. Valluchi, C.; Sippel, M.: Hypersonic Morphing for the SpaceLiner Cabin Escape System, 7th European Conference for Aeronautics and Space Sciences (EUCASS), Milan 2017
32. Stappert, S.; Sippel, M.; Bussler, L.; Wilken, J.; Krummen, S.: SpaceLiner Cabin Escape System Design and Simulation of Emergency Separation from its Winged Stage, AIAA 2018-5255, 22nd AIAA International Space Planes and Hypersonic Systems and Technologies Conference, 17-19 September 2018, Orlando, Florida, USA
33. Bayrak, Y.M.: Multi-body Simulation of the SpaceLiner Cabin Rescue System, SART TN-009/2019, October 2019
34. Wilken, J.: SpaceLiner System Specification Document, SL-SS-SART-00026-1/1, SART TN-003/2018
35. Bussler, L; Karl, S.; Sippel, M.: Shock-Shock Interference Analysis for SpaceLiner Booster, 2nd HiSST: International Conference on High-Speed Vehicle Science Technology, Bruges, September 2022
36. Sippel, M. et al: Enhancing Critical RLV-technologies: Testing Reusable Cryo-Tank Insulations, IAC-19-D2.5.10, 70th International Astronautical Congress, Washington 2019
37. Wilken, J. et al: Testing combined cryogenic insulation and thermal protection systems for reusable stages, IAC-21-D2.5.4, Dubai 2021
38. Reimer, T.; Rauh, C.; Di Martino, G.D.; Sippel, M.: Thermal Investigation of a Purged Insulation System for a Reusable Cryogenic Tank, Journal of Spacecraft and Rockets, 59 (4), p. 1205-1213, https://doi.org/10.2514/1.A35252
39. Wilken, J.; et al: Critical Analysis of SpaceX's Next Generation Space Transportation System: Starship and Super Heavy, 2nd HiSST: International Conference on High-Speed Vehicle Science Technology, Bruges, September 2022
40. Bussler, L; Sippel, M.; von Rüden, D.F.: Reference Concept SLB 8 Booster, AKIRA report R-2004, SART TN-001/2020, March 2020
41. Sippel, M.; Stappert, S.; Callsen, S.; Dietlein, I.; Bergmann, K.; Gülhan, A.; Marquardt, P., Lassmann, J.; Hagemann, G.; Froebel, L.; Wolf, M.; Plebuch, A.: A viable and sustainable European path into space – for cargo and astronauts, IAC-21-D2.4.4, 72nd International Astronautical Congress (IAC), Dubai, 25-29 October2021, Download Link
42. Stappert, S., Sippel, M., Callsen, S., Bussler, L.: Concept 4: A Reusable Heavy-Lift Winged Launch Vehicle using the In-Air-Capturing method, 2nd HiSST: International Conference on High-Speed Vehicle Science Technology, September 2022, Bruges, Belgium
43. Blank, J.; Deb, K: pymoo: Multi-Objective Optimization in Python, in IEEE Access, vol. 8, pp. 89497-89509, 2020, doi: 10.1109/ACCESS.2020.2990567
44. Deb, K.; Jain, H.: An evolutionary many-objective optimization algorithm using reference-point-based nondominated sorting approach, Part I: solving problems with box constraints, IEEE Transactions on Evolutionary Computation, 18(4):577–601, 2014, doi:10.1109/TEVC.2013.2281535
45. Jain, H.; Deb, K.: An evolutionary many-objective optimization algorithm using reference-point based nondominated sorting approach, Part II: handling constraints and extending to an adaptive approach. IEEE Transactions on Evolutionary Computation, 18(4):602–622, August 2014
46. Sippel, M., Wilken, J., Callsen, S.; Bussler, L.: Towards the next step: SpaceLiner 8 pre-definition, IAC-23-D2.4.2, 74th International Astronautical Congress (IAC), Baku, Azerbaijan, 2023, Download Link
47. Mauriello, T.: Multidisciplinary Design Analysis & Optimization of the SpaceLiner Passenger Stage, SART TN-014/2023, 2023

Further updated information concerning the SART space transportation concepts is available at:
http://www.dlr.de/SART